NAVAL POSTGRADUATE SCHOOL

MONTEREY, CALIFORNIA

THESIS

FACTORS CONTRIBUTING TO THE INTERRUPTED DECAY OF HURRICANE JOAQUIN (2015) IN A MODERATE VERTICAL WIND SHEAR ENVIRONMENT

by

Adam C. Jorgensen

June 2017

Thesis Advisor: Eric Hendricks
Second Reader: Russell Elsberry

Approved for public release. Distribution is unlimited.

THIS PAGE INTENTIONALLY LEFT BLANK

REPORT DOCUMENTATION PAGE		*Form Approved OMB No. 0704–0188*
Public reporting burden for this collection of information is estimated to average 1 hour per response, including the time for reviewing instruction, searching existing data sources, gathering and maintaining the data needed, and completing and reviewing the collection of information. Send comments regarding this burden estimate or any other aspect of this collection of information, including suggestions for reducing this burden, to Washington headquarters Services, Directorate for Information Operations and Reports, 1215 Jefferson Davis Highway, Suite 1204, Arlington, VA 22202-4302, and to the Office of Management and Budget, Paperwork Reduction Project (0704-0188) Washington, DC 20503.		
1. AGENCY USE ONLY *(Leave blank)*	**2. REPORT DATE** June 2017	**3. REPORT TYPE AND DATES COVERED** Master's thesis
4. TITLE AND SUBTITLE FACTORS CONTRIBUTING TO THE INTERRUPTED DECAY OF HURRICANE JOAQUIN (2015) IN A MODERATE VERTICAL WIND SHEAR ENVIRONMENT		**5. FUNDING NUMBERS**
6. AUTHOR(S) Adam C. Jorgensen		
7. PERFORMING ORGANIZATION NAME(S) AND ADDRESS(ES) Naval Postgraduate School Monterey, CA 93943-5000		**8. PERFORMING ORGANIZATION REPORT NUMBER**
9. SPONSORING /MONITORING AGENCY NAME(S) AND ADDRESS(ES) N/A		**10. SPONSORING / MONITORING AGENCY REPORT NUMBER**
11. SUPPLEMENTARY NOTES The views expressed in this thesis are those of the author and do not reflect the official policy or position of the Department of Defense or the U.S. Government. IRB number ___N/A____ .		
12a. DISTRIBUTION / AVAILABILITY STATEMENT Approved for public release. Distribution is unlimited.		**12b. DISTRIBUTION CODE**

13. ABSTRACT (maximum 200 words)

This study investigates the environmental factors and the internal processes that contributed to the interrupted rapid decay of Hurricane Joaquin (2015). In-situ data from the Office of Naval Research (ONR) Tropical Cyclone Intensity (TCI) field campaign, global and regional analyses, and satellite and microwave imagery provides a detailed picture of the environment surrounding Joaquin as well as the inner-core region during this period. Additionally, a special dataset comprised of 15-minute temporal frequency vertical wind shear values calculated from rapid-scan atmospheric motion vectors provides an unprecedented look at the high spatial and temporal frequency nature of vertical wind shear, and its role on TC structure and intensity change. Utilization of the high temporal and spatial resolution dropsonde datasets allowed calculations of the vertical tilt of Joaquin to investigate the internal processes. Vertical wind shear and environmental analysis for Hurricane Joaquin discloses a situation in which a major hurricane was able to interrupt a rapid decay based primarily on the relaxation of vertical wind shear, which allowed it to re-align in the low- to mid-troposphere. Further use of the 15-minute VWS calculations to model such a dynamic environmental factor should greatly aid models in accurately forecasting intensity and structure changes.

14. SUBJECT TERMS tropical cyclone, hurricane, Joaquin, vertical wind shear			**15. NUMBER OF PAGES** 97
			16. PRICE CODE
17. SECURITY CLASSIFICATION OF REPORT Unclassified	**18. SECURITY CLASSIFICATION OF THIS PAGE** Unclassified	**19. SECURITY CLASSIFICATION OF ABSTRACT** Unclassified	**20. LIMITATION OF ABSTRACT** UU

i

THIS PAGE INTENTIONALLY LEFT BLANK

FACTORS CONTRIBUTING TO THE INTERRUPTED DECAY OF HURRICANE JOAQUIN (2015) IN A MODERATE VERTICAL WIND SHEAR ENVIRONMENT

Adam C. Jorgensen
Lieutenant, United States Navy
B.S., Principia College, 2006

Submitted in partial fulfillment of the
requirements for the degree of

MASTER OF SCIENCE IN METEOROLOGY AND PHYSICAL OCEANOGRAPHY

from the

**NAVAL POSTGRADUATE SCHOOL
June 2017**

Approved by: Eric Hendricks
                Thesis Advisor

                Russell Elsberry
                Second Reader

                Wendell Nuss
                Chair, Department of Meteorology

THIS PAGE INTENTIONALLY LEFT BLANK

ABSTRACT

This study investigates the environmental factors and the internal processes that contributed to the interrupted rapid decay of Hurricane Joaquin (2015). In-situ data from the Office of Naval Research (ONR) Tropical Cyclone Intensity (TCI) field campaign, global and regional analyses, and satellite and microwave imagery provides a detailed picture of the environment surrounding Joaquin as well as the inner-core region during this period. Additionally, a special dataset comprised of 15-minute temporal frequency vertical wind shear values calculated from rapid-scan atmospheric motion vectors provides an unprecedented look at the high spatial and temporal frequency nature of vertical wind shear, and its role on TC structure and intensity change. Utilization of the high temporal and spatial resolution dropsonde datasets allowed calculations of the vertical tilt of Joaquin to investigate the internal processes. Vertical wind shear and environmental analysis for Hurricane Joaquin discloses a situation in which a major hurricane was able to interrupt a rapid decay based primarily on the relaxation of vertical wind shear, which allowed it to re-align in the low- to mid-troposphere. Further use of the 15-minute VWS calculations to model such a dynamic environmental factor should greatly aid models in accurately forecasting intensity and structure changes.

THIS PAGE INTENTIONALLY LEFT BLANK

TABLE OF CONTENTS

LIST OF FIGURES

LIST OF TABLES

THIS PAGE INTENTIONALLY LEFT BLANK

LIST OF ACRONYMS AND ABBREVIATIONS

ADD	Automated Dropsonde Dispenser
AMV	atmospheric motion vector
ATL	Atlantic basin
CIMSS	Cooperative Institute for Meteorological Satellite Studies
CIRA	Cooperative Institute for Research in the Atmosphere
DOD	Department of Defense
DON	Department of the Navy
DTG	date time group
EOL	Earth Observing Laboratory
GFS	Global Forecast System
GPS	Global Positioning System
GOES	Geostationary Operational Environmental Satellite
HDSS	High-Definition Sounding System
HIRAD	Hurricane Imaging Radiometer
Hz	Hertz
I	intensifying
IR	Infrared
km	kilometer
kt	knot
m/s	meters per second
MEMS	Microelectromechanical System
MSLP	mean sea level pressure
MTCSWA	multi-platform tropical cyclone surface wind analysis
MTSAT	Multifunctional Transport Satellite
N	neutral
NASA	National Aeronautics and Space Administration
NCEP	National Centers for Environmental Prediction
NESDIS	National Environmental Satellite, Data and Information Service
NHC	National Hurricane Center

NM	nautical miles
NWS	National Weather Service
ONR	Office of Naval Research
PV	potential vorticity
RAMMB	Regional and Mesoscale Meteorology Branch
RH	relative humidity
RI	rapidly intensifying
SFMR	Stepped Frequency Microwave Radiometer
SHIPS	Statistical Hurricane Intensity Prediction System
SST	sea surface temperature
TC	tropical cyclone
TCI	Tropical Cyclone Intensity
Theta-e	potential temperature
UTC	Coordinated Universal Time
VR	vortex removed
VNR	vortex not removed
VRW	vortex Rossby Waves
VWS	vertical wind shear
W	weakening
WWOSC	World Weather Open Science Conference
XDD	eXpendable Digital Dropsonde
ZWC	zero wind center

ACKNOWLEDGMENTS

THIS PAGE INTENTIONALLY LEFT BLANK

I. INTRODUCTION

A. MOTIVATION

Hurricane Joaquin (2015) was the strongest Atlantic hurricane of non-tropical origin in the satellite era (Berg 2016). Besides being a non-traditional major hurricane because of where it formed, it exhibited another unique trait rarely seen in tropical cyclone (TC) life cycles. On 4 October 2015, a rapid decay of the storm was interrupted and then Joaquin maintained intensity for 30 hours in a moderate vertical wind shear (VWS) environment. A moderate VWS environment is defined as wind shear magnitude between 5 and 10 m/s (Corbosiero and Molinari 2002). Normally, moderate VWS is not conducive to extending a hurricane's life cycle, much less anticipating a constant intensity in that type of environment. Due to this anomalous behavior, forecasters were unable to accurately predict the intensity during this extended life-time of Hurricane Joaquin.

The motivation of this thesis is to discover what combination of environmental factors (sea surface temperature (SST), relative humidity (RH), vertical wind shear (VWS), and divergence aloft and internal processes (e.g., vortex tilt in response to the VWS, and surface wind evolution in the eye wall region) were responsible for the interrupted rapid decay of Hurricane Joaquin. Providing an accurate depiction of the environment around the storm as well as at the core is critical to investigating the factors that prompted the interruption of the rapid decay. The availability of new and improved datasets and diagnostic tools should give a level of detail to all aspects of the storm never before realized.

In addition to the environmental datasets above, the Office of Naval Research (ONR) Tropical Cyclone Intensity (TCI) field experiment provided an unprecedented in-situ dataset to study internal processes within Hurricane Joaquin and investigate the impact of these processes on TC intensity change.

1

During the TCI field campaign in 2015, the WB-57 aircraft flew over Hurricane Joaquin at an altitude of approximately 60,000 ft (~18,000 meters) and deployed dropwindsondes into the storm from the High Definition Sounding System (HDSS). These new in-situ observations will be used to understand the kinematic and thermodynamic structure of a TC in vertical wind shear.

A third unique opportunity for this thesis will be the utilization of the Zero-Wind-Center (ZWC) tool created by Creasey and Elsberry (2017). Using the HDSS dropsonde data from the TCI-15 field program, the tool uses the wind directions observed at different levels as the dropsonde falls to the surface to triangulate the storm center positions to a high degree of accuracy from the upper levels to the surface. As indicated in Creasey and Elsberry (2017), investigating the tilt of the Joaquin vortex could provide answers as to how Joaquin responded to the environmental VWS.

B.   OBJECTIVE

The specific questions to be investigated in this study of Hurricane Joaquin are: What environmental VWS changes and/or internal processes led to the interruption of the rapid decay of the storm, but then allowed a period of constant intensity? Are there insights that can be gleaned from this storm that can be applied to future storms to increase the accuracy of intensity forecasts in moderate VWS? Investigation of environmental factors such as sea-surface temperatures under the storm center, the orientation of the outflow boundary in the upper levels, and other associated synoptic features that either facilitate or inhibit storm intensification are anticipated to increase understanding of the dynamics that impact intensity change.

The specific focus of this thesis is an investigation of upper-level outflow processes and dynamics of Hurricane Joaquin utilizing data collected during the TCI-15 field experiment datasets. The TCI field program, in addition to the HDSS dropsondes deployed from the National Aeronautics and Space Administration (NASA) WB-57 aircraft, utilized the NASA Hurricane Imaging Radiometer

(HIRAD) on the WB-57 to measure the surface wind speed and rain rate. A special atmospheric motion vector (AMV) dataset at 15-minute intervals will be utilized to describe the environmental VWS conditions around Hurricane Joaquin.

The objective of studying the interrupted decay of Joaquin with the standard environmental datasets and these special TCI-15 field experiment observations is to better understand the dynamic nature of the response of Joaquin to environmental VWS from top to bottom.

C.   NAVAL RELEVANCE

There are both scientific and military benefits to be gained from this research. For the scientific community, while it is well known that strong VWS decreases the intensity, and weak VWS is favorable for intensification, less is known about the impacts of *moderate* VWS on TC intensity change. Additionally, the specific internal mechanisms by which a TC can resist moderate VWS is not well known. For the military, the most important takeaway from this research for the Department of the Navy (DON) and the Department of Defense (DOD) will be the potential for improved accuracy and precision in future forecasts of TC intensity change in vertical wind shear. Such improvements will bring about greater confidence in the forecast intensity of hurricanes, which will both optimize the safety of Fleet Operations. In addition, millions of dollars in fuel or repair costs may be saved in the event of a coastal hurricane when the military leadership has to decide based on intensity and track forecasts, whether to keep the Fleet in port or deploy to sea to avoid damage.

THIS PAGE INTENTIONALLY LEFT BLANK

II.   BACKGROUND

It is well known that strong VWS is usually detrimental to the development and intensification of a TC (DeMaria 1996; Frank and Ritchie 2001; Rios-Berrios and Torn 2017). As technological advances have led to improved observations of the inner structure of the vortex, this effect of VWS has become even more apparent. Velden and Sears (2014) and Rios-Berrios and Torn (2017) indicate the range of VWS magnitudes that cause significant impacts to TC structure and intensity is 5-15 m/s. Any VWS greater than 15 m/s will quickly and dramatically weaken a TC.

While VWS is defined by the instantaneous vertical derivative of the velocity vector at any height, for tropical cyclones the deep-layer change in the velocity vector over the entire troposphere is commonly used as the metric for assessing its effect on hurricane intensity. Thus, the most widely used deep-layer VWS computation is the difference of the velocity vector between 200 mb and 850 mb. This two-level vector difference is commonly used, for example in the Statistical Hurricane Intensity Prediction Scheme (SHIPS) (DeMaria et al. 2004). The magnitude of this deep-layer wind shear at a given latitude and longitude is

$$VWS = \left| \overrightarrow{U_{200}} - \overrightarrow{U_{850}} \right|,$$

where U_{200} is the velocity vector at 200 mb and U_{850} is the velocity vector at 850 mb. The difference of these velocity vectors represents the environmental VWS vector at a given latitude and longitude. One advantage to this method is the simplicity of the calculation. Another advantage is that these wind vectors for the VWS calculation are readily available from global model analyses or forecast fields. Using the two-level method is especially useful in the operational environment when access to high-frequency, rapid-scan satellite imagery for calculating Atmospheric Motion Vectors (AMVs) is often limited.

Elsberry and Jeffries (1996) and Velden and Sears (2014) suggest a potential disadvantage with the above two-level VWS calculation (Figure 1). Although the two estimates of VWS in Figures 1a and 1b would be similar, the dynamic impact of these wind profiles in the vertical on a TC would be very different. Whereas the impact of VWS in Figure 1a would be an interaction primarily with the TC outflow layer, the impact of the VWS in Figure 1b would be on all levels of the TC.
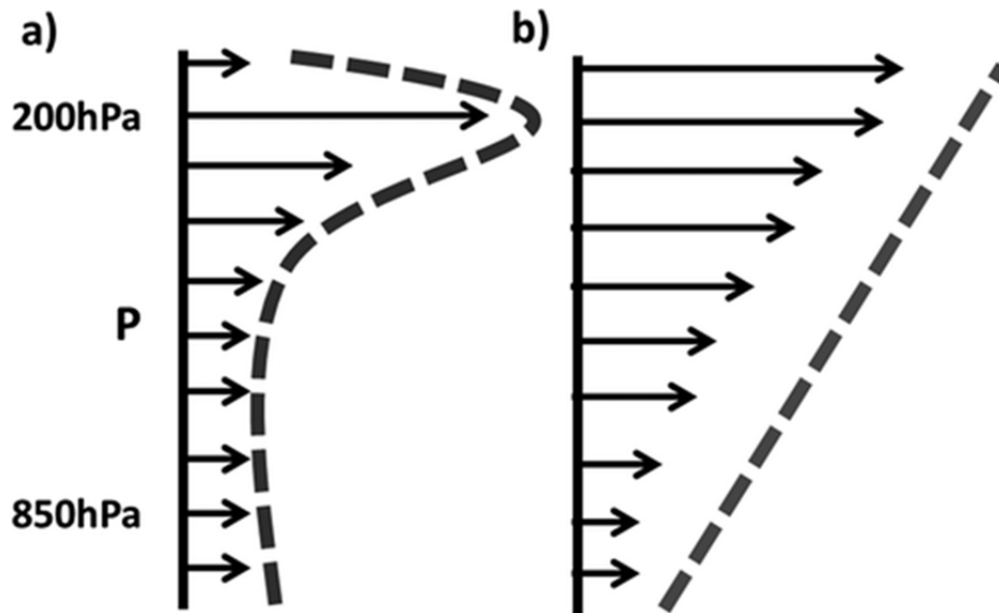
Two different wind profiles in the vertical that return the same VWS value using the two-level SHIPS-based calculation. The right panel indicates shear induced by a trough while the left panel indicates shear induced by a ridge. Adapted from Elsberry and Jeffries (1996); Velden and Sears (2014).

Figure 1. Vertical Wind Profiles that Return the Same VWS Value Using the Two-Level Calculation.

Velden and Sears (2014) have recently improved the calculation of VWS based on AMVs from the Cooperative Institute for Meteorological Satellite Studies (CIMSS). This advance in tropical analyses and diagnostics came along with the automation process for generating high-density AMV datasets between

150 and 300 mb based on the abundance of cirrus clouds and a secondary maximum below 700 mb associated with shallow convective clouds (Velden and Sears 2014). The CIMSS deep-layer shear calculation method differs from the standard two-level method in that layer averages are used from 950–700 mb and 300–150 mb, to encapsulate more details of the vertical variation in the horizontal velocity vector with height.

The advantage of the CIMSS VWS calculation is that it provides an average velocity vector in the upper layer and an average velocity vector in the lower layer to detect a vertical structure such as in Figure 1a versus Figure 1b. There is still uncertainty in the mid-levels, but the use of low and upper level average winds may improve the VWS calculation.

The disadvantages of the CIMSS VWS calculation stem from the complexity of the AMV calculations, the computing power required to run the calculation, and the availability of information in band-width limited environments. Note that low-level AMVs will generally not be available under a very dense cloud shield. The CIMSS VWS calculation is based on locally produced wind analyses and requires a three-dimensional recursive filter at high spatial resolution, with larger analysis weights given to available high-density satellite-derived winds. From a production standpoint, the computing power at CIMSS is not a concern, but the resultant files are so data-intensive they may be problematic for operational military entities.

A.   VWS IMPACTS ON HURRICANES

A number of negative and positive factors may impact hurricane development, maturation and sustainability. The four common negative VWS impacts from Davis and Chan (2014) summary of the World Weather Open Science Conference (WWOSC-2014) includes: (i) filamentation of the upper-tropospheric piece of the potential vorticity (PV) monolith (Frank and Ritchie 2001); (ii) ventilation of the mid-troposphere (Gray 1968; Tang

and Emanuel 2010); (iii) subsidence induced over the low-level center of a tilted vortex (DeMaria 1996); and (iv) ventilation of the boundary layer inflow (Riemer et al. 2010).

Considering first the filamentation of the upper-tropospheric PV monolith from Frank and Ritchie (2001), the importance of a vertically aligned, axisymmetric structure to maintain the intensity of a storm in the presence of VWS cannot be overstated. Filamentation, in this case, is the intrusion of VWS in thin bands that cause the warm air and potential vorticities to dissipate (Frank and Ritchie 2001). The PV monolith terminology arises since TCs typically have a large area of PV in the center that extends a large distance in the troposphere and which decays moving radially outward. The three proposed mechanisms are filamentation, eyewall instability, and turbulent mixing. The hypothesis is that those three mechanisms combine to maintain the PV maxima and the equivalent potential temperature maxima. If the TC becomes asymmetric due to VWS, these three mechanisms may not be able to sustain the balance within the TC to maintain intensity. Instability develops that result in the warm core over the storm as well as the central PV anomaly being advected away. Even though this instability starts in the upper levels where the vortex is weakest, the dissipation of the warm core aloft will also from hydrostatic consideration increase the surface pressure and thus weaken the storm (Frank and Ritchie 2001).

Examining the VWS impact mechanism leading to ventilation of the mid-troposphere as hypothesized by Gray (1968) and Tang and Emanuel (2010), the potential vorticity column becomes tilted due to differential advection by the background flow. The subsequent excitation of asymmetries interacting with the power generation of the TC vortex no longer constrains the heat energy relative to the TC center. One of the hypotheses proposed by Tang and Emanuel (2010) is that low entropy environmental air at mid-levels is forced into the eyewall by eddies. Injection of this low entropy air into the eyewall decreases the total

amount of work that can be performed by the TC to combat frictional dissipation, which leads to an overall weakening of the storm.

The third theory proposed by DeMaria (1996) is that when environmental upper-layer winds differ from the lower-layer winds, the potential vorticity associated with the vortex circulation becomes tilted in the vertical, which requires a larger mid-level temperature perturbation near the vortex center to maintain the balanced mass field. Since warming in the mid-levels increases the low-level static stability, convective activity is reduced and the TC development is inhibited. As the upper-layer PV is displaced from the low-level PV, a weakening of the mid-level temperature perturbation occurs in the direction of the vortex vertical tilt. As these eddies pull more energy out of the eyewall, this could increase convection away from the storm center, which further tilts the vortex away from vertical.

Finally, Reimer et al. (2010) postulate that environmental VWS may lead to a ventilation of the boundary layer inflow. That is, strong and persistent shear-induced downdrafts may force low equivalent potential temperature (theta-e) air into the boundary layer from above, which will dilute the theta-e values in the TC inflow layer. As this lower theta-e air enters the eyewall updrafts, this will lower the temperature of the eyewall, and therefore the available energy for convection. These low theta-e downdrafts may be formed due to a convective asymmetry outside the eyewall that sometimes extends to a radius of 150 km. Such vortex scale downdrafts form when precipitation falls from a sloped updraft into the unsaturated air below and evaporates. The Reimer et al. (2010) numerical simulation, as well as some observational data, provides good support that the inflow interaction with the boundary layer could very well negatively impact the intensity of the storm by the introduction of low theta-e air.

In contrast to these negative impacts of VWS on the development and intensification of TCs, there are hypotheses as to an intrinsic resiliency mechanism for the TC vortex to resist shear. Thus, the concept of vortex resiliency and its influence of the outflow on VWS also needs to be considered.

According to Reasor et al. (2004), vortex Rossby Waves (VRWs) have a fundamental role in TC vortex resiliency. A dry and adiabatic inviscid damping mechanism was identified associated with VRWs that suppressed departures from an upright state. Vortex resiliency is the ability to maintain vortex vertical alignment while withstanding VWS greater than 10 m/s over the depth of the troposphere. However, diabatic processes augment the efficiency of the VRW damping mechanism in reducing the tilt of the TC vortex. The strengthening of VWS causes VRWs to strengthen, providing an intrinsic alignment mechanism. If the VRWs are sufficiently strong, the vortex can re-align by counter acting the differential advection of the TC by VWS (Reasor et al. 2004). The precession frequency of the vortex is another critical factor in vortex resiliency. That is, the greater the vortex precession frequency, the more resilient the vortex will be to differential advection by the VWS (Jones 1995; Reasor et al. 2004).

Little published research exists on the influence that the TC outflow has on VWS. However, a number of dependencies exist between these two environmental factors: (i) Relative strength of the VWS compared to the outflow; (ii) Orientation of the VWS compared to the orientation of the outflow; (iii) since outflow occurs in a thin layer at the top of the TC, a TC may be able to better resist the VWS profile from an anticyclone (Figure 1a) as opposed to a trough (Figure 1b). Given a strong outflow boundary and only moderate VWS, it is possible that the upper-level flow contributing to that moderate VWS may be incorporated into the outflow which would decrease the impact of the VWS on the

upper levels of the vortex. In that case, the VWS may not be inhibited by the strong outflow boundary and the TC outflow may be sheared apart or its course be significantly altered.

B.   SYNOPTIC OVERVIEW OF HURRICANE JOAQUIN

Based on the synoptic description in the National Hurricane Center (NHC) Tropical Cyclone Report (Berg 2016), initial development of Hurricane Joaquin began on 8 September west-southwest of the Canary Islands in conjunction with the development of a weak upper-tropospheric low. However, intensification did not occur until three weeks later (0600 UTC 29 September) when the system had translated westward to near 27°N, 70°W (Figure 2). Joaquin underwent rapid intensification and became a major hurricane (Category 3) at 0000 UTC 01 October (Figure 2 inset). Sea-surface temperatures were approximately 1.1°C higher than normal and were the warmest on record which was favorable for Joaquin maintaining major hurricane strength until 1200 UTC 4 October. However, increasing northwesterly VWS then eroded the western eyewall which caused the storm to weaken. A deep low located over the southeastern United States provided the steering mechanism to turn Joaquin to the north-northeast 4 October and this translation direction continued until 5 October. As Joaquin continued to track northeastward and then east-northeastward it became embedded in the mid-latitude westerlies. The combination of increased VWS and colder ocean temperatures precipitated the decrease of Joaquin to a tropical storm at 1200 UTC 7 October.

One of the striking features of Hurricane Joaquin was the interruption of the extreme decay at 1800 UTC 4 October, and then its maintenance of a constant intensity of 75 kt from 0000 UTC 5 October through 0600 UTC 6 October (Table 1). Whereas post-recurvature hurricanes typically decay as they move poleward over colder water, the 70 kt decay from maximum intensity of 135 kt at 1200 UTC 3 October to 65 kt just 30 hours later is an extreme decay

rate. Then to re-intensify to 75 kt and maintain that intensity for 30 hours while accelerating poleward is quite unusual. This period of interrupted rapid decay followed by constant intensity is the focus of this thesis.
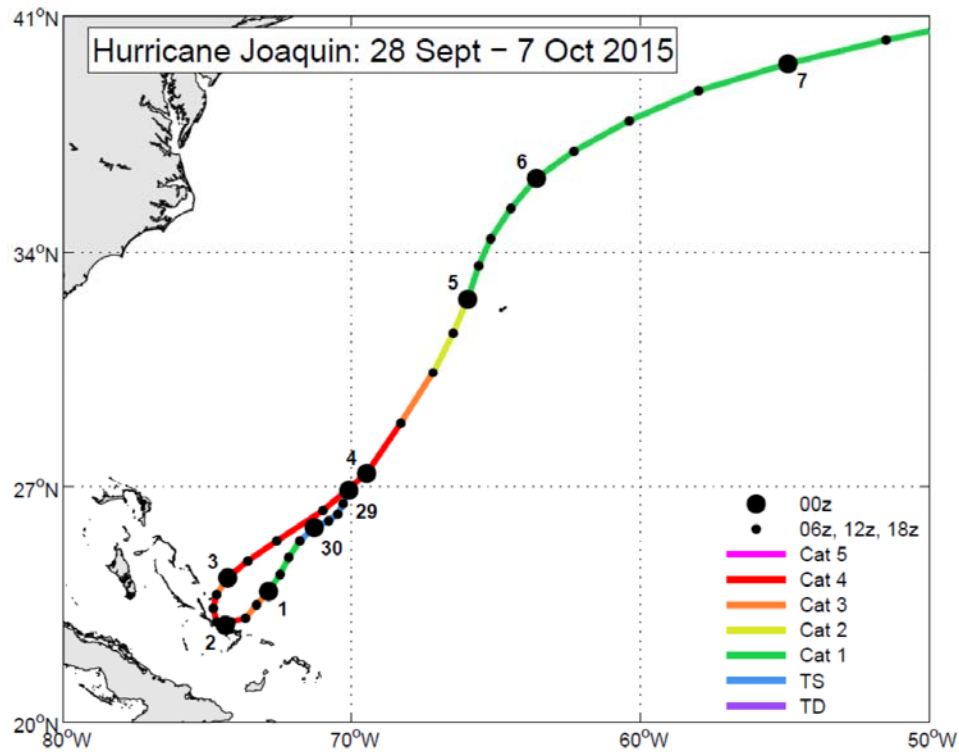
Best track positions and storm stages (see color in inset) for Hurricane Joaquin. Source: NHC, Doyle et al. (2017).

Figure 2. NHC Best Track Positions and Intensities for Hurricane Joaquin.

Table 1.　　Time, Location and Intensity of Hurricane Joaquin.

DTG	Latitude	Longitude	Pressure	Wind Speed (kt)	Classification
02 / 0000	22.9	74.4	931	120	Hurricane
02 / 0600	23	74.7	935	120	"
02 / 1200	23.4	74.8	937	115	"
02 / 1600	23.6	74.8	940	110	"
02 / 1800	23.8	74.7	941	110	"
02 / 2100	24.1	74.5	942	110	"
03 / 0000	24.3	74.3	943	115	"
03 / 0600	24.8	73.6	945	120	"
03 / 1200	25.4	72.6	934	135	"
03 / 1800	26.3	71	934	130	"
04 / 0000	27.4	69.5	941	115	"
04 / 0600	28.9	68.3	949	105	"
04 / 1200	30.4	67.2	956	95	"
04 / 1800	31.6	66.5	958	65	"
05 / 0000	32.6	66	961	75	"
05 / 0600	33.6	65.6	964	75	"
05 / 1200	34.4	65.2	964	75	"
05 / 1800	35.3	64.5	964	75	"
06 / 0000	36.2	63.6	967	75	"
06 / 0600	37	62.3	970	75	"
06 / 1200	37.9	60.4	974	70	"

Date Time Group (DTG), latitude, longitude, central pressure and sustained winds for Hurricane Joaquin before, during and after the interrupted decay as seen between 05/0000 and 06/0600. Adapted from Berg (2016).

C.　　TCI MISSIONS INTO HURRICANE JOAQUIN

The purpose of the ONR-funded TCI-15 field experiment was to improve the prediction of TC intensity and structure change by utilizing a NASA WB-57 equipped with HDSS to deploy eXpendable Digital Dropsondes (XDD) to take environmental measurements as they fall through TCs. The NASA WB-57 was also equipped with HIRAD designed to remotely measure ocean surface wind speeds and rain rates.

The TCI-15 field program flew successful NASA WB-57 missions over Hurricane Joaquin from Macon, Georgia on four consecutive days (2–5 October). Take-off time was typically around 1500 UTC, and the four flight tracks are shown in Figure 3 overlaid on a montage of Hurricane Joaquin images from Geostationary Operational Environmental Satellite (GOES). Except for 5 October, each mission included two overpasses of the eye of the storm as well as intersecting the outflow on the inbound and outbound segments.
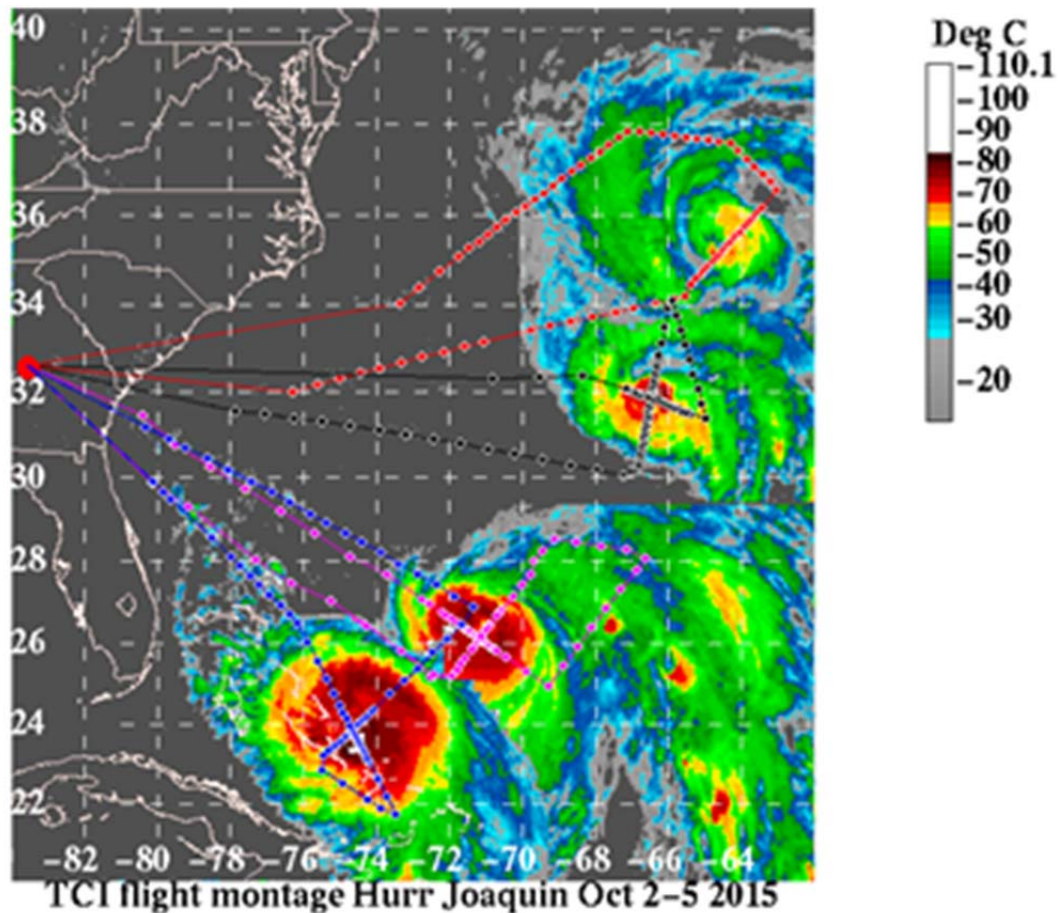
WB-57 flight track (solid line) and dropsonde launch locations (diamonds) for the four TCI flights over Joaquin, overlaid on GOES infrared satellite imagery, with each image centered on the time the aircraft was over the storm. Source: Doyle et al. (2017).

Figure 3. TCI Flight Montage 2-5 October 2015.

14

During the 2 October mission, Hurricane Joaquin had an asymmetric eyewall with the largest brightness temperatures along the southern periphery of the eye (Figure 4).
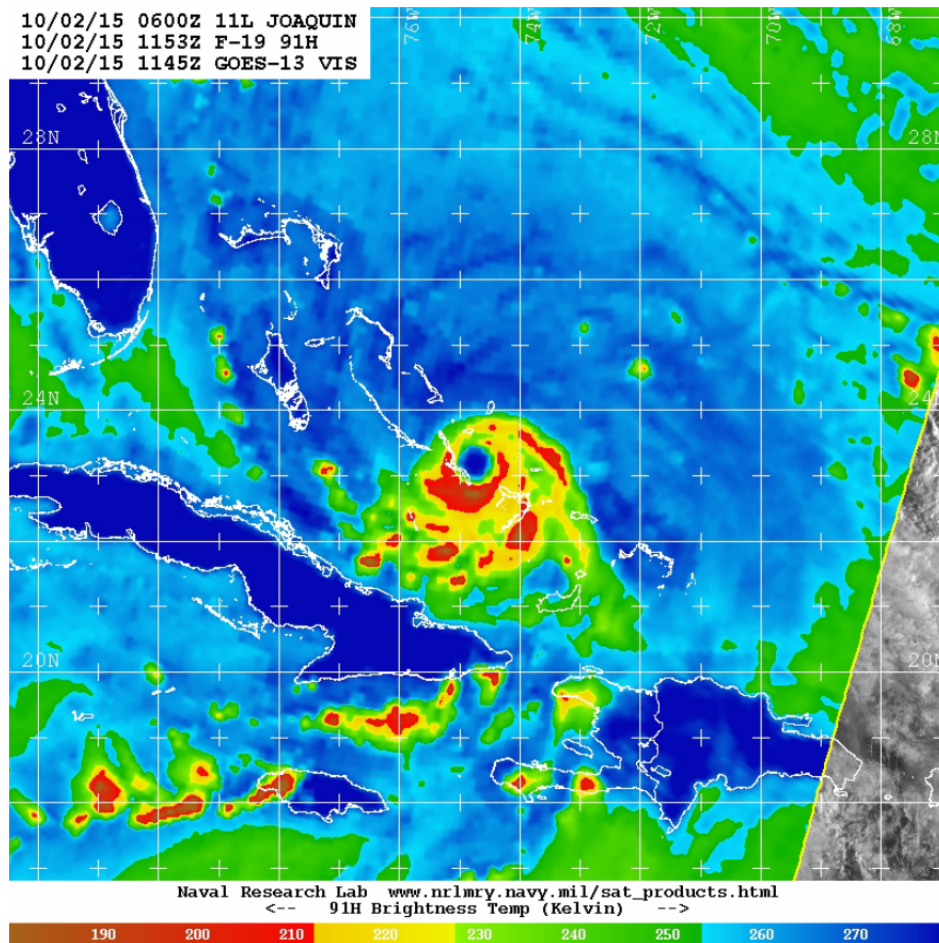
Geostationary satellite infrared (IR) imagery at 1145 UTC 2 October 2015 showing the brightness temperatures (Kelvin, color bar at bottom) and the asymmetric deep convection around the eye of Joaquin. Source: Naval Research Laboratory (2015).

Figure 4. NRL IR Imagery Showing Brightness Temperature and Asymmetric Deep Convection around Hurricane Joaquin.

Notice the asymmetry in the convection in the southern hemisphere of the inner-core region of Joaquin.
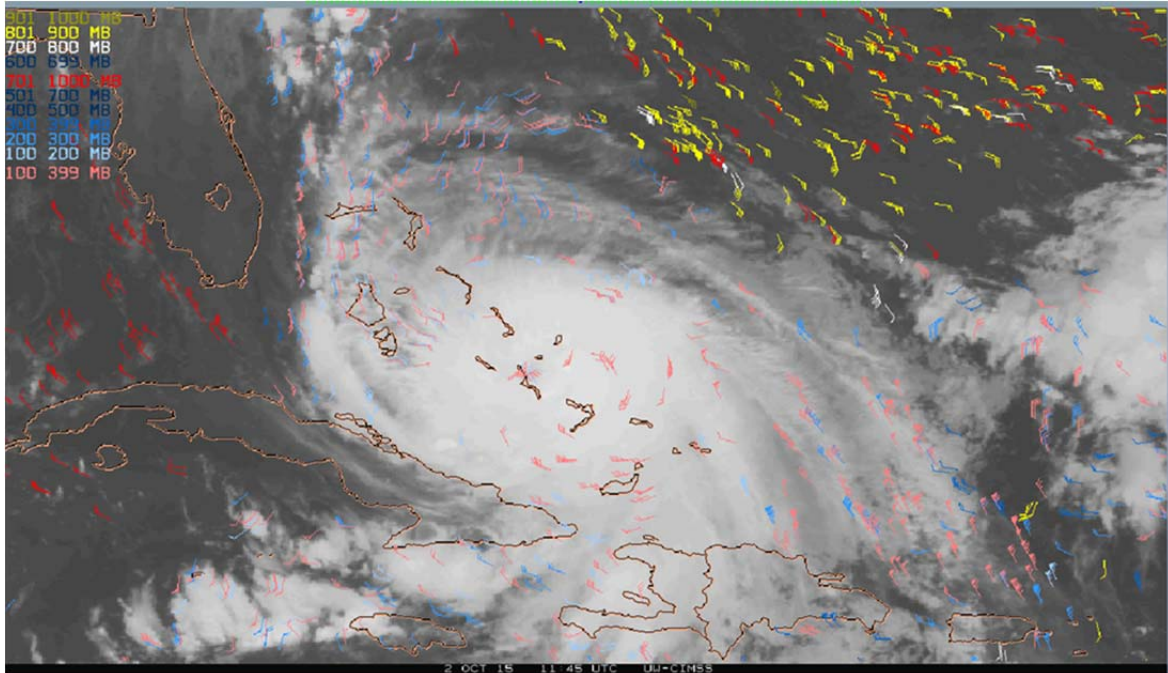
1145 UTC 2 October AMVs zoomed in around Hurricane Joaquin. Pink wind barbs indicate 100–399 mb VWS average magnitude and direction while red wind barbs indicate 701–1000 mb VWS average magnitude and direction. Courtesy of Chris Velden, UW-CIMSS.

Figure 5. 1145 UTC 2 October AMVs

The 1145 UTC 2 October AMVs have a very dense cloud deck that makes it very hard for the CIMSS VWS algorithm to pinpoint lower-level motion in the inner-core of Joaquin (Figure 5). The AMVs pinpoint two outflow jets, one equatorward on the east side of Joaquin and one poleward on the west side of Joaquin. The poleward out flow jet has linked up with the trough over the eastern United States.

The Global Forecast System (GFS) 200 mb streamline and isotach analysis shows a very deep, mid-latitude upper-level trough moving eastward across the eastern United States (Figure 6) to the east of Hurricane Joaquin, which is over the northern Bahama Islands. There is also a sub-tropical upper-tropospheric trough near 30°N, 60°W.
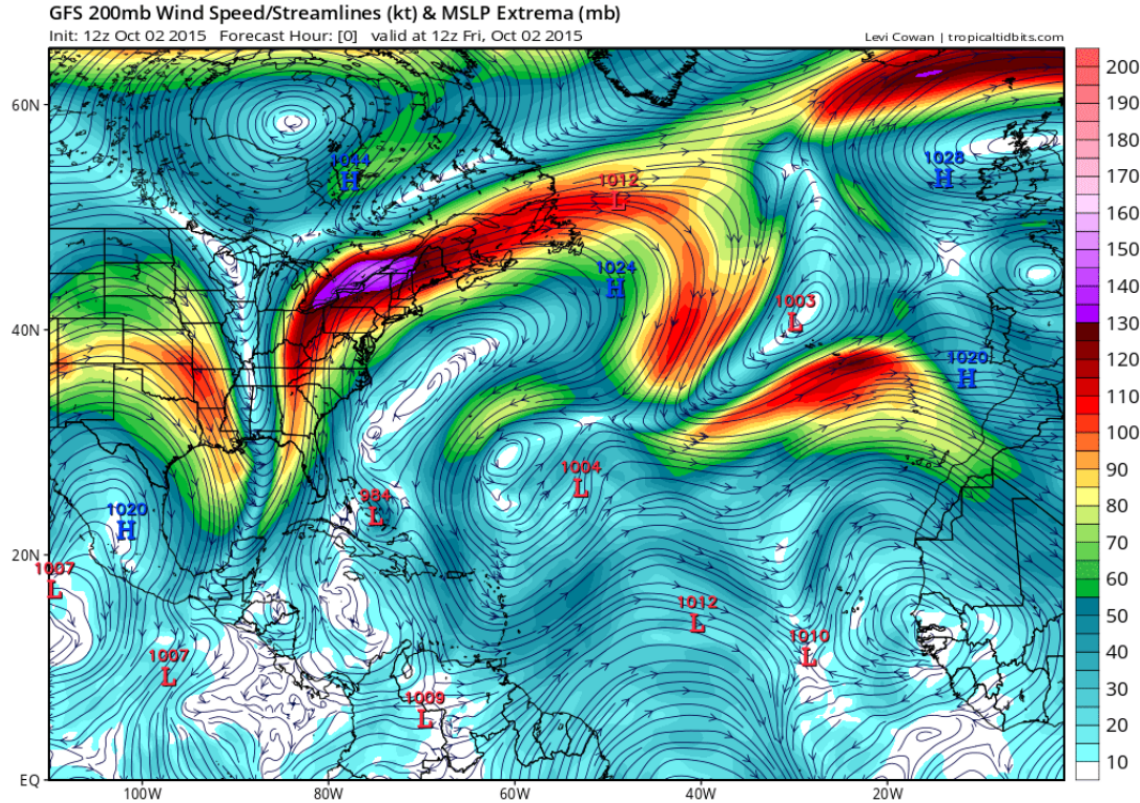
Global Forecast System (GFS) 200 mb streamlines and isotachs (m/s, color scale on right) and MSLP lows (red 'L') at 1200 UTC 2 October 2015. Source: Levi Cowan, tropicaltidbits.com (n.d.)

Figure 6. GFS Isotachs and MSLP 1200 UTC 2 October 2015

Dropsondes deployed from the NASA WB-57 around the periphery of Joaquin (not shown) at 1604 UTC 2 October generally has an inversion around 950 mb and then a saturated environment up to 675 mb with winds being primarily from the south throughout the sounding. The tilt of the vortex was observed to be toward the south-southwest by the onboard scientist based on convective activity, which is consistent with the higher brightness temperatures in that region (Figure 4).

The 3 October mission departed Macon, Georgia at 1500 UTC, flew southeastward (Figure 3) to over-fly Hurricane Joaquin around 1800 UTC, which was near 26°N, 71°W and near maximum intensity (Table 1). Geostationary IR satellite imagery at 1515 UTC 3 October (Figure 7) indicates well the tiny eye of Joaquin. Note that convection has completely wrapped around the eye with the strongest convection in the western semicircle, even though no deep convection is occurring farther west.
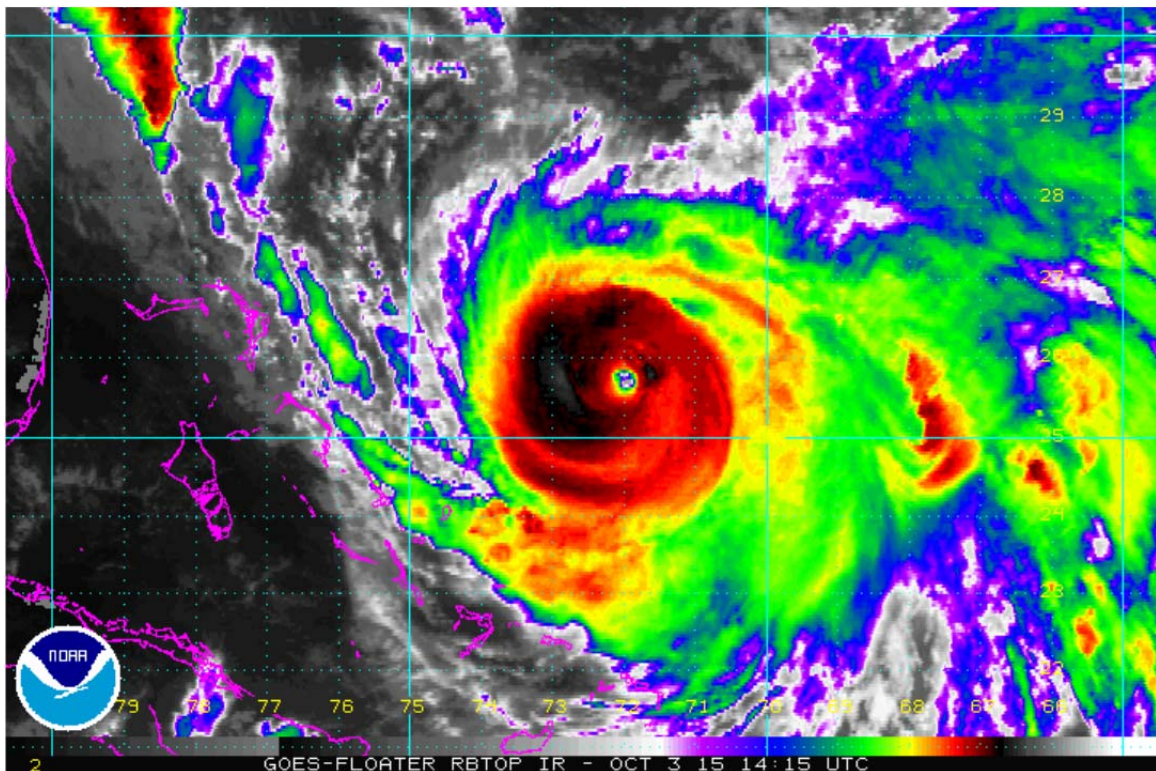
Geostationary satellite infrared imagery of Hurricane Joaquin at 1515 UTC 3 October. Notice the strongest convection has shifted from the southern periphery of Joaquin to the western semicircle. Source: NOAA (n.d.).

Figure 7. GOES IR Imagery of Hurricane Joaquin at 1415 UTC 3 October

As indicated by the eye position in Figure 7, Joaquin had begun to move to the northeast away from the Bahama Islands (Figure 2) and at 1800 UTC 3 October was at 26.3°N, 71°W (Table 1).
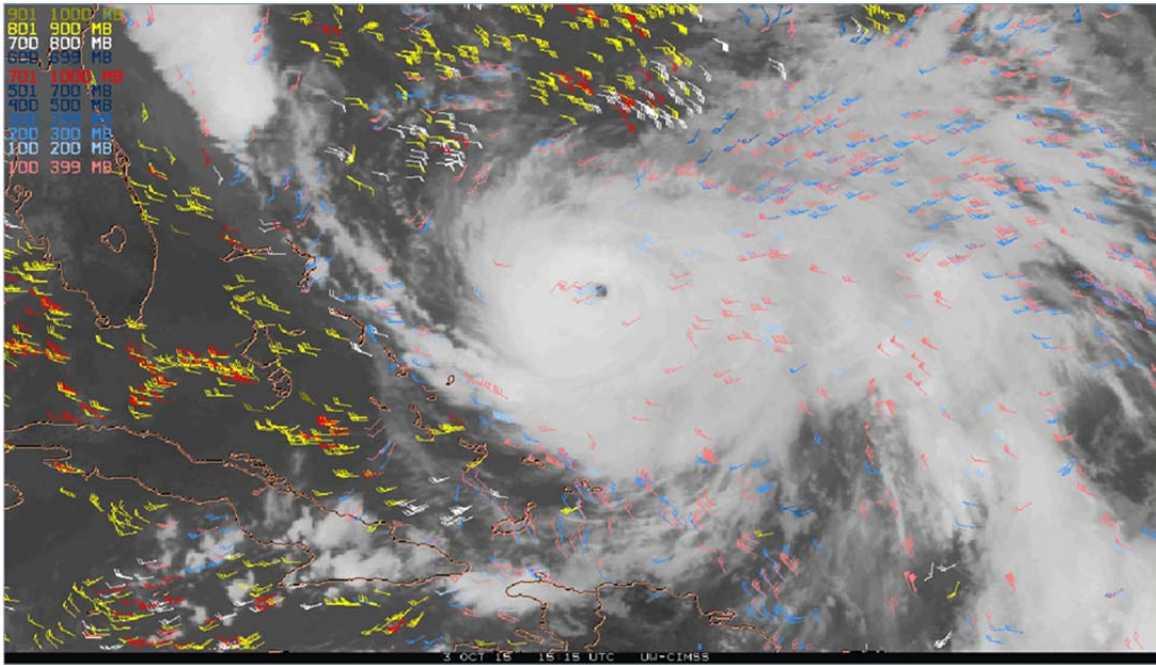

1515 UTC 3 October AMVs zoomed in around Hurricane Joaquin. Pink wind barbs indicate 100–399 mb VWS average magnitude and direction while red wind barbs indicate 701–1000 mb VWS average magnitude and direction. Courtesy of Chris Velden, UW-CIMSS.

Figure 8. 1515 UTC 3 October AMVs

The 1515 UTC 3 October AMVs again show sporadic upper-level VWS layer averages but are lacking lower-level VWS layer averages due to heavy clouds. The outflow jets have shifted, the poleward jet oriented just off the coast of Florida and the equatorward jet has shifted to the northeast quadrant of Joaquin and is almost zonal in its orientation.

The GFS analysis at 250 mb at 1800 UTC (Figure 9) indicates the deep mid-latitude trough in Figure 6 had advanced eastward over Florida. Furthermore, the upper-tropospheric low that had been to the east of Joaquin was now to the north near 34°N, 70°W. Thus, the upper-tropospheric steering

flow across Joaquin was now toward the northeast. GOES infrared imagery at 1837 UTC (not shown) suggests a vortex tilt from southwest to northeast that is consistent with this upper-tropospheric steering flow.
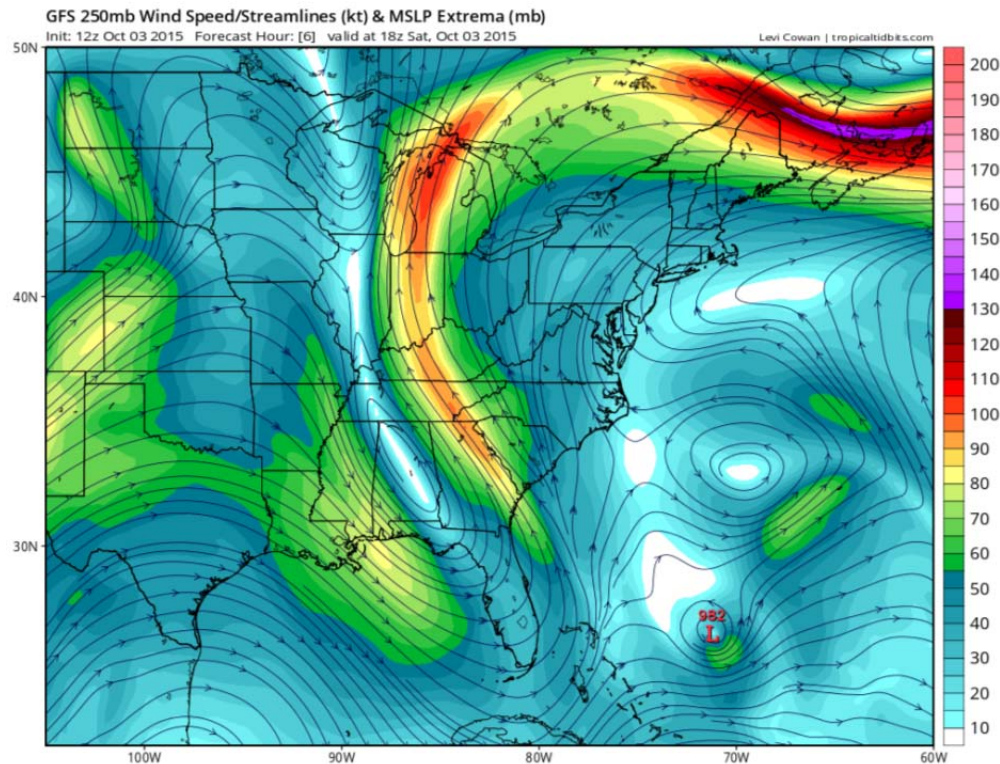

Global Forecast System (GFS) 250 mb streamlines and isotachs (m/s, color scale on right) and MSLP lows (red 'L') at 1800 UTC 3 October 2015. Source: Levi Cowan, tropicaltidbits.com.

Figure 9. GFS Isotachs and MSLP 1800 UTC 3 October 2015

The 4 October mission departed, Macon, Georgia, at 1527 UTC and flew eastward along 30°N to then overpass Hurricane Joaquin at 1800 UTC from the south (Figure 3). After a second center overpass from the east at 1900 UTC, the NASA WB-57 exited the storm along 35°N. At 1800 UTC 4 October the intensity of Joaquin had decreased to 65 kt and was located near 31.6°N, 66.5°W (Table 1).

GOES IR imagery at 1445 UTC 4 October (Figure 10) indicates the deep convection in Joaquin had been radically deformed during the previous 24 hours

since the imagery at 1515 UTC 3 October (Figure 7). Although there is a closed eyewall, almost all deep convection is to the north of the eye so that the convection is highly asymmetric. Indeed, the absence of deep convection to the southwest of the eye is consistent with a strong southwest–to–northeast flow across Joaquin at upper levels on 3 October (Figure 9). The CIMSS analysis of VWS (described earlier in Chapter II) does show a southwest–to–northeast shear across Joaquin at 1800 UTC (not shown). By 1845 UTC, the GOES imagery did not have a distinguishable eye (not shown).
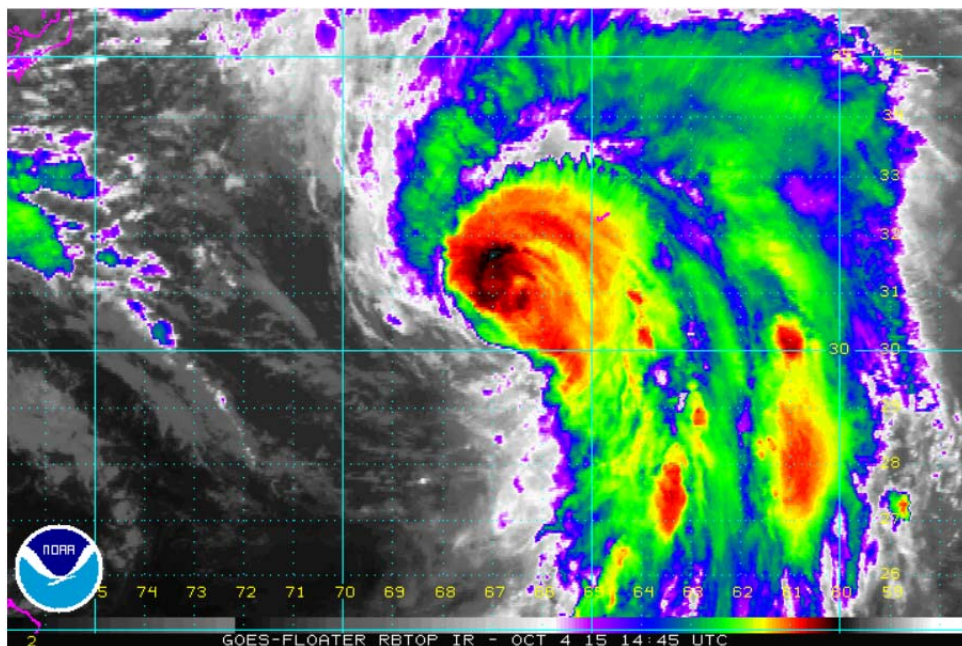
Geostatics satellite IR imagery of Hurricane Joaquin at 1445 UTC 4 October. Joaquin has become radically deformed under the effects of VWS. Source: NOAA (n.d.).

Figure 10.   GOES IR Imagery of Hurricane Joaquin at 1445 UTC 4 October

The 1445 UTC 4 October AMVs provide a strong return for low- to mid-level winds to the southwest of Joaquin (Figure 11). It appears that the poleward outflow jet has been cutoff and the equatorward outflow jet has weakened considerably as it is oriented almost directly north-south as Joaquin continues to

be deformed under the influence of strong (13.3 m/s CIMSS, 12.6 m/s SHIPS) VWS from the southwest.
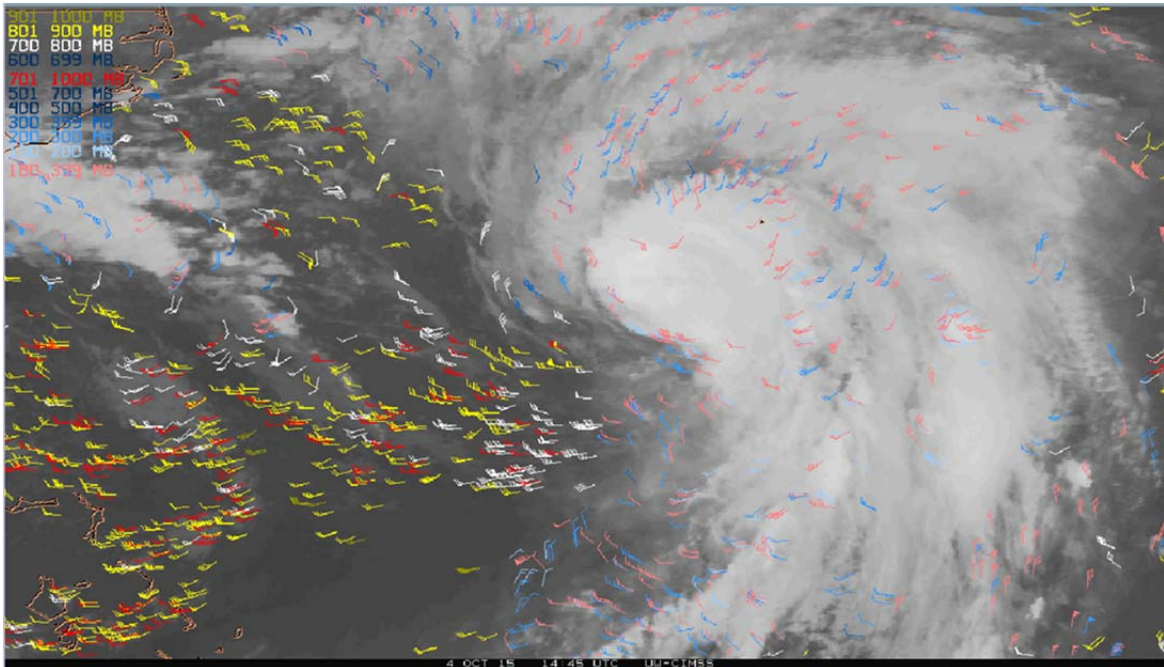
1445 UTC 4 October AMVs zoomed in around Hurricane Joaquin. Pink wind barbs indicate 100–399 mb VWS average magnitude and direction while red wind barbs indicate 701–1000 mb VWS average magnitude and direction. Courtesy of Chris Velden, UW-CIMSS.

Figure 11.   1515 UTC 3 October AMVs

Finally, the 5 October mission departed Macon, Georgia at 1448 UTC and flew to the east-northeast (Figure 3) to observe Joaquin which had moved rapidly to the northeast on 4 October (Figure 2) and at 1800 UTC 5 October was near 35.3°N, 64.5°W with an intensity of 75 kt (Table 1). Given the long transit to the storm, only a single southwest–to–northeast overpass of the center was possible (Figure 3).

The GOES IR imagery at 1445 UTC 5 October (Figure 12) indicated that the convection in Joaquin had become more organized with an enshrouded eye and rainbands spiraling outward on the western and northern sides as expected in a hurricane. The sea-surface temperature was still around 27°C, which is

considered still favorable for hurricane-force winds. The GFS 200 mb streamline/isotach analysis at 1800 UTC 5 October (not shown) indicates that Joaquin was still embedded in southwesterly winds aloft. The CIMSS VWS had diminished to approximately 6 m/s (not shown), which is considered to be moderate VWS (Velden and Sears 2014) for the hurricane stage.
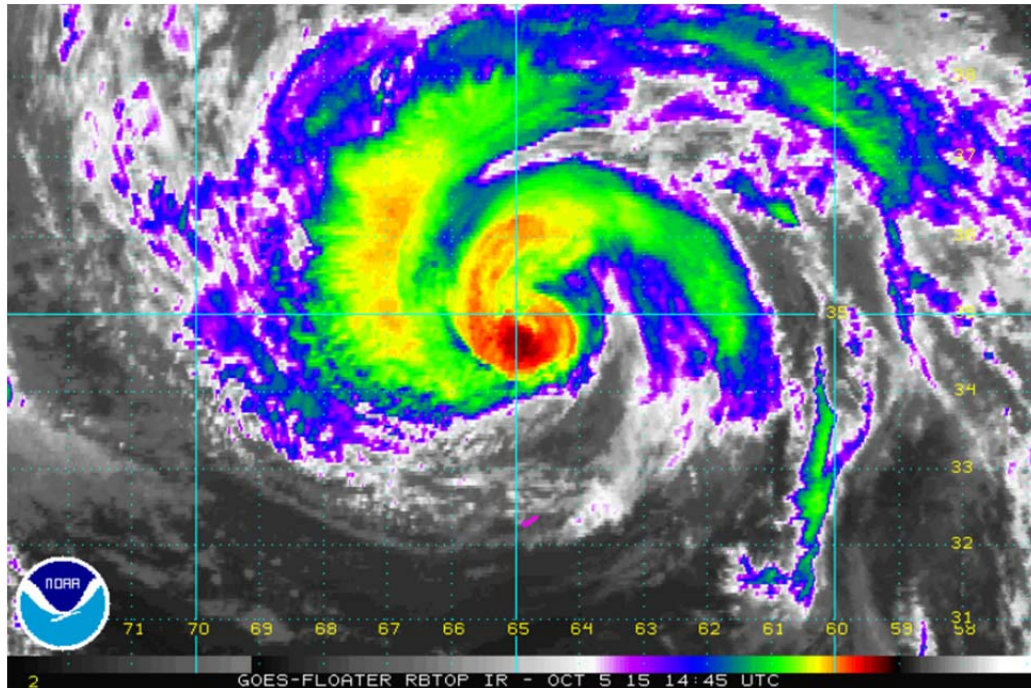
Geostationary satellite IR imagery of Hurricane Joaquin at 1445 UTC 5 October. Joaquin has continued to weaken. Source: NOAA (n.d.).

Figure 12.   GOES IR Imagery of Hurricane Joaquin at 1445 UTC 5 October

After the onset of the interrupted rapid decay, Joaquin has become better organized (Figure 13). The poleward outflow jet has emerged, oriented northwest to southeast on Joaquin's western side. The equatorward outflow jet is still oriented in the northeast quadrant but now wraps more tightly around the storm.
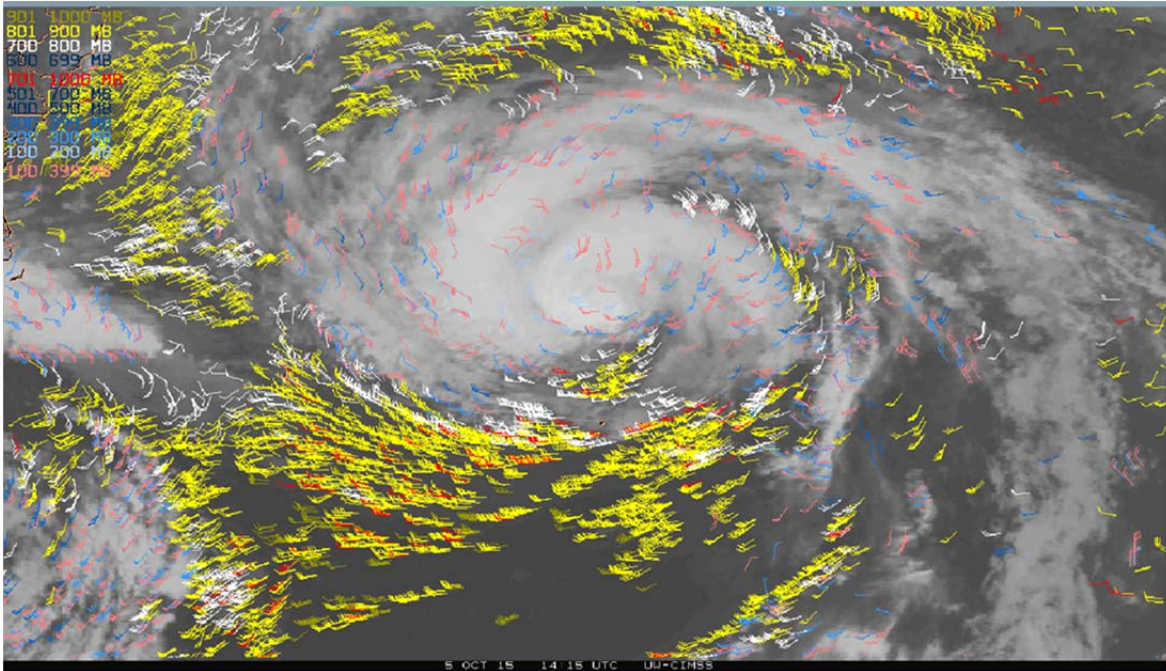
23

1445 UTC 4 October AMVs zoomed in around Hurricane Joaquin. Pink wind barbs indicate 100–399 mb VWS average magnitude and direction while red wind barbs indicate 701–1000 mb VWS average magnitude and direction. Courtesy of Chris Velden, UW-CIMSS.

Figure 13.   1145 UTC 2 October AMVs

GOES East wind shear shows south-southwestward shear between 10 and 20 knots. GFS 200 mb winds show Joaquin in an area of southwesterly winds, in agreement with the CIMSS derived wind analyses. The sea surface temperature is still around 27°C; not ideal for maintaining intensity, but not yet cold enough to induce significant weakening. Deep layer shear had also relaxed to approximately 6 m/s.

No flight was conducted on 6 October due to Joaquin being out of range for another NASA WB-57 mission. Note that the intensity of Joaquin was still 75 kt at 0600 UTC 6 October (Table 1).

III. DATA AND METHODOLOGY

A. TCI FIELD PROGRAM

The purpose of the ONR-funded TCI-15 initiative was to improve the prediction of TC intensity and structure change by paying special attention to the characteristic that TC outflow jets tend to be directed preferentially in different quadrants based on the nature of the environmental interactions (Doyle et al. 2017). Due to the complex relationships between the storm and environment, more observations are required to improve the accuracy of TC intensity and structure forecasts. Unique datasets were obtained during the TCI-15 field experiment by the deployment of HDSS with the Yankee XDD. Deploying these dropsondes from the NASA WB-57 flying at 60,000 feet (~18,000 meters) in and around four TCs has produced in-situ high temporal and spatial resolution observations to aid in quantitative analysis of TC intensity and structure.

A total of four missions were successfully made by the NASA WB-57 aircraft over and around Hurricane Joaquin between 2 and 5 October. The methodology in this thesis is to examine the HDSS datasets collected during the TCI-15 field experiment in conjunction with satellite and environmental analysis data to explain the interrupted rapid decay of Joaquin on 4 October and then the constant intensity in a moderate VWS environment.

B. DATA

1. High Definition Sounding System (HDSS)

The HDSS is an integrated system of antennas, receivers, and telemetry that receives data from XDDs deployed by the Automated Dropsonde Dispenser (ADD) (Black et al. 2017). These datasets consist of GPS location, altitude, air temperature, pressure, relative humidity, horizontal wind speed and direction, and the sea-surface temperature upon splashdown. The sensor specifications are summarized in Table 2.

Table 2.   XDD Sensor Specifications

Parameter	Sensor type/data rate	Range	Accuracy	Resolution
Temperature	Thermistor/2 Hz/1 Hz[a]	-90° to 50°C	±0.14°C	0.016°C
Pressure	MEMS[b]/2–1 Hz[a]	150–1150 mb	±1.5 mb at 25°C	±2.5 mb
Humidity	MEMS[b]/2–1 Hz[a]	10%–100% for temp >-37°C	1.8% at 25°C	0.1%
Sea surface temperature	Infrared micro-radiometer, 9–11 µm/1 Hz	0°–50°C	±0.2° at 25°C	0.016°C

[a] Early sonde data rate for Twin Otter and DC-8 flights
[b] MEMS: Microelectromechanical System

Parameters measured by the XDD dropsonde system by various sensors, and the range, accuracy, and resolution of these measurements. Adapted from Black et al. (2017).

The XDDs were launched from the NASA WB-57 at an altitude of approximately 60,000 feet (~18,000 meters) to fall through the TC outflow and the eyewall of the storm to gain insight into the dynamic processes impacting TC intensity and structure. While some issues of sensor freezing occurred at the high altitudes in TCI-15 impacting upper-level wind, relative humidity, air temperature, and potentially sea surface temperature (SST) measurements, overall the sensors performed very well. The comparisons with National Weather Service (NWS) radiosondes and RD-94 dropsondes indicated biases of 1° C warmer and approximately 5% drier (Black et al., 2017). The mid-wing, long-range WB-57 aircraft proved to be an optimal platform for deploying the HDSS dropsondes from 60,000 feet (~18,000 meters) through TCs. The WB-57 range of 2,500 nautical miles (nm) was sometimes a limitation, but the long-range planning by the TCI-15 team and the exceptional cooperation by the WB-57 pilots and support team led to these unique observations in Joaquin.

2.   HIRAD Data

As explained in Doyle et al. (2017), HIRAD is a C-band synthetic thinned-array passive microwave radiometer that uses a retrieval concept similar to the operational Stepped Frequency Microwave Radiometer (SFMR). HIRAD provides a 50–70 km wide swath of surface wind speeds and rain rates along the WB-57 flight path for each of the 2 to 5 October missions. The surface wind speed is

related to the near-blackbody emissions from foam on the roughened ocean surface. This data will be utilized to investigate how vortex surface winds are changing in response to the VWS. Since HIRAD will provide the surface wind speed but is unable to provide wind direction, the Global Positioning System (GPS)-positions of the HDSS sondes as they fall will be utilized to derive wind directions.

3. Regional and Mesoscale Meteorology Branch (RAMMB) Analysis

In order to maximize the available surface level wind information, the RAMMB surface wind analysis will be utilized. The analysis of the inner core is determined almost completely by aircraft input with the multi-platform tropical cyclone surface wind analysis (MTCSWA) used as a first guess field while the outer regions are determined by blending aircraft observations with MTCSWA (RAMMB 2017).

4. Special CIMSS 15-Minute Vertical Wind Shear Datasets

Atmospheric Motion Vectors (AMVs) are derived by tracking the motion of cloud tops or water vapor features via geostationary satellite images. Velden and Sears (2014) describe the Cooperative Institute for Meteorological Satellite Studies (CIMSS) processing algorithm for deriving AMVs over TCs, which is similar to the operational algorithm and approach used by National Environmental Satellite, Data and Information Service (NESDIS). The Global Forecast System (GFS) analyses are used for the sophisticated AMV height assignment and post-processing routines. These AMV datasets are derived hourly using satellite imagery from GOES, Meteosat, and Multifunctional Transport Satellites (MTSATs). In addition to visualizing wind fields around TCs, these AMVs provide insight into the dynamical processes at different levels. In support of the TCI-15 analyses, the CIMSS provided a special dataset of 15-minute interval AMVs that provides a unique opportunity to more closely track the wind fields at different levels at high temporal frequency. The algorithm for

generating the CIMSS wind fields is described in Velden and Sears (2014) as follows: the appropriate AMVs are gridded onto zonal and meridional wind fields detailed in Velden et al. (1998). An objective analysis using a three-dimensional recursive filter weighs AMVs in the assimilation process (Velden et al. 1998, 2005). The background fields are provided by the operational National Centers for Environmental Prediction (NCEP) Global Forecast System (GFS) model. Two sets of 15-minute gridded fields were provided by CIMSS for Joaquin: one with the GFS tropical cyclone vortex removed, and one without the vortex removed. These will be discussed in more details in the next section.

5. SHIPS/CIMSS 6-Hourly Vertical Wind Shear and SHIPS Environmental Datasets

The Statistical Hurricane Intensity Prediction Scheme (SHIPS) calculates the VWS slightly differently than CIMSS. Instead of using the mean of two layers, it simply employs the GFS analyses at 200 and 850 mb. After removing the symmetric TC vortex flow from each field, in the SHIPS method, an average vector difference within a radial distance of 500 km from the TC center (Velden and Sears 2014) is calculated. This SHIPS 6-hour VWS dataset will be examined as a background to the 15-minute interval CIMSS dataset that will provide higher temporal resolution regarding the evolution of the VWS around Hurricane Joaquin during the rapid decay and the interruption to become a constant intensity.

The SHIPS analyses will also be used to investigate the magnitude of other environmental impacts on the storm. These include a vortex-removed deep-layer VWS and an annulus (vortex not removed) deep-layer VWS. In addition to these different VWS values, the SHIPS dataset provides operational analysis values for the sea-surface temperature (SST), upper-level divergence, relative humidity, maximum winds, and environmental vorticity. The averaging areas for divergence and vorticity are 0–1000 km while SST, relative humidity, and maximum winds are averaged over an annulus with radius from

200–800 km. The inner circle was determined based on the typical differences between the NHC official track and the GFS track out to three days (DeMaria et al. 2005).

C.   ANALYSIS

1.   Zero-Wind-Center (ZWC) Tool

Because the TCI-15 field program was focused on observing the extreme gradients of wind, pressure, temperature, and dew point temperature across the inner-core region, the HDSS dropsondes provided an excellent dataset for calculating the zero-wind center (ZWC) positions of Joaquin (Creasey and Elsberry 2017). Creasey and Elsberry calculated average wind directions over 1-km layers from the GPS readings received from the XDD as the dropsonde descended from 60,000 ft (~18,000 meters) to the ocean surface. They modified the technique of Willoughby and Chelmow (1982) for constructing a sequence of normal vectors to these wind directions to define the ZWC at 200m intervals. An advantage of calculating the ZWCs from two overpasses of the eye is that the sonde data can be put into a storm-relative coordinate system. Determining the position of the storm at the first sonde drop is crucial to correctly identifying the storm-relative coordinate system. After these two ZWCs are calculated, Creasey and Elsberry developed an iterative procedure that determines the speed and direction the vortex has translated.

2.   Horizontal Averaging Methods

There are two main schools of thought for averaging VWS around TCs. As explained in Rhome et al. (2005), the first is based on a user-established radius that is dependent on the size of the storm. The impetus for this approach was to attempt to remove the symmetric portion of the TC circulation. However, if the storm is not axisymmetric, this simple radius method will include some of the VWS of the storm as well as the surrounding environment. With the arrival of GFS in 2001 this became more complicated because it included a representation of a TC (DeMaria et al. 2005). It became necessary to remove the circulation

from the grid and interpolate and reassign values based on the surrounding environmental wind information and the VWS is calculated out to a radius of 500 km. The second method was to leave the TC circulation in place and use an annulus with an inner radius of 200 km and an outer radius of 800 km to minimize contamination of the environmental VWS due to the TC circulation (Velden and Sears 2014). The first method is referred to here as Vortex Removed (VR) and the second method is referred to as Vortex Not Removed (VNR).

IV.   ENVIRONMENTAL FACTORS AFFECTING TC INTENSITY

A.   6-HOURLY SHIPS ENVIRONMENTAL DATA ANALYSIS

In order to better understand the environmental factors that may have contributed to the interrupted decay of Hurricane Joaquin, the intensity in terms of both V_{max} and mean sea level pressure (MSLP) between 0000 UTC 3 October and 0000 UTC 6 October, is shown in Figure 14. Peak intensity for this time period was reached at 1200 UTC 3 October with maximum winds of 135 knots (kt) and minimum sea-level pressure of 934 millibars (mb). The time frame for the interrupted decay was 0000 UTC 5 October to 0000 UTC 6 October when Joaquin had filled and then stabilized at 964 mb, and the maximum wind speed remained at 75 knots for a 24-hour period. It is noteworthy to mention that Joaquin maintained an essentially constant intensity out to 0000 UTC 7 October (MSLP measured 974 mb and maximum winds were 70 kt) (Berg 2016). However, the rapid decay that occurred from 1200 UTC 3 October and 1200 UTC 4 October will also be examined in terms of environmental factors such as strong VWS.

MSLP (mb, blue line) and Maximum Winds (knots, red line) for Hurricane Joaquin between 0000 UTC 3 October and 0000 UTC 6 October from the NHC best-track file. Source: Berg (2016).

Figure 14.   NHC Best Track MSLP and Maximum Winds

The real-time SHIPS synoptic time analyses (DeMaria et al. 2005) will be used to investigate the environmental factors in the vicinity of Hurricane Joaquin. The hypothesis is that the VWS changes are the critical factor to determining the interrupted rapid decay.

First, the deep-layer VWS is analyzed using two different methods. As described in Chapter III.B.4-5, the SHIPS method uses a vector difference of the 200 mb to 850 mb winds around the TC vortex as an estimate for the deep-layer VWS, while the CIMSS method relies more heavily on AMVs and also uses lower and upper troposphere layer averages. These SHIPS analyses will be compared with the 6-hourly CIMSS wind analyses.

The magnitudes of the deep-layer VWS calculated from SHIPS and CIMSS analyses have some immediately noticeable differences (Figure 15). The magnitude of the VWS provided by SHIPS is at times considerably lower than the magnitude of VWS provided by CIMSS. Averaged throughout the 3–6 October period, the CIMSS VWS magnitude is approximately 3.3 m/s larger than the SHIPS VWS magnitude. As stated in DeMaria et al. (2005), the SHIPS VWS is calculated within an annulus radius 200–800 km that avoids the uncertainty due to the storm center location and the high winds. However, there are still large fluctuations between synoptic times in the SHIPS VWS magnitudes. There is also a slight, but not insignificant, difference in average VWS direction between the SHIPS and CIMSS datasets (Figure 15, right panel). Generally, there is good agreement through 1200 UTC 5 October between SHIPS and CIMSS directions. However, a noticeable difference between the two VWS directions occurred at 1800 UTC 5 October, with the SHIPS VWS having a more west-southwesterly orientation while the CIMSS VWS had a southwesterly orientation. At 0000 UTC 6 October, the SHIPS VWS had shifted to just west of southwest and the CIMSS VWS shifted to a more southerly direction.
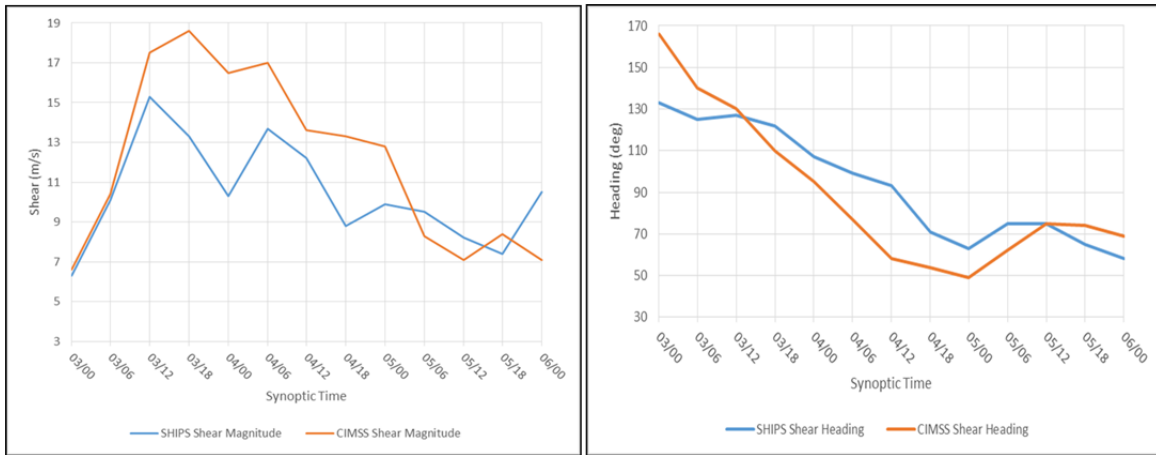
SHIPS (blue line) and CIMSS (orange line) 6-hourly VWS magnitude (m/s, left panel) and direction (deg, right panel) toward which the VWS vector is pointed before and during the interrupted decay period.

Figure 15. SHIPS and CIMSS Vortex Removed Re-analysis VWS Magnitude and Direction

Another environmental contribution to the interrupted rapid decay of Hurricane Joaquin may have been changes in the sea-surface temperatures (SSTs) (Figure 16). Nyoumura and Yamashita (1984) concluded that TC intensification is more likely to occur over SSTs higher than 28°C. As might be expected from the northeastward storm track of Joaquin between 0000 UTC 3 October and 0000 UTC 6 October (Figure 2) the SST drops below 28°C at 1800 UTC 4 October and continues to decrease for the remainder of the study period (Figure 16).

DeMaria and Kaplan (1993) indicated that the tropopause temperature will also be higher when the TC has recurved to be over a SST of 26°C compared to when the TC had been over the tropical ocean with a SST of 29°C. That is, the atmospheric column over a SST of 26°C will be cooler and shallower. Therefore, the MSLP of the TC will be higher and the TC will tend to weaken. According to this argument, the SST should decrease along the track of Joaquin and contribute to the weakening of Joaquin, and thus is the SST changes are not the cause of the interrupted rapid decay of Joaquin.
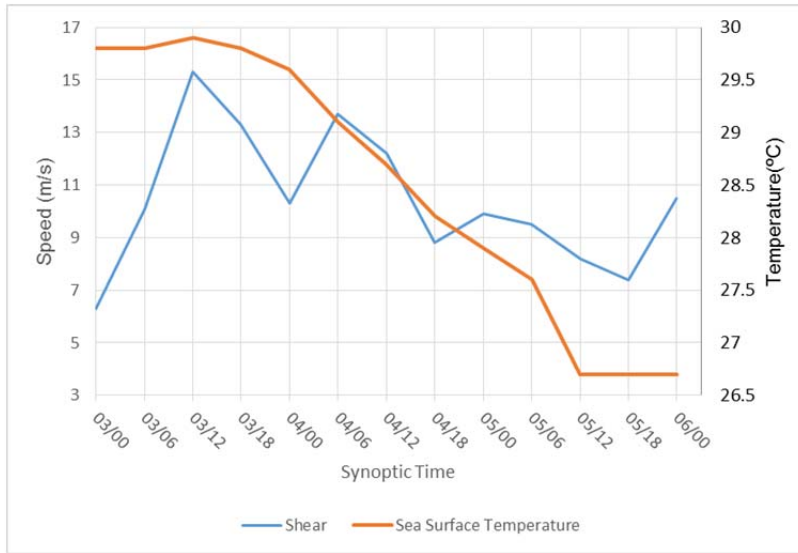
6-hourly VWS magnitude (m/s, blue line) as in Figure 11 (left panel) from SHIPS with real-time analysis sea surface temperature (°C, orange line).

Figure 16.   SHIPS VWS and SHIPS Sea Surface Temperature

The intensity of any TC may be related to the magnitude of the divergence aloft (Bosart et al. 2000). The divergence aloft is due to air exiting the deep convection in the inner-core and moving radially outward, and thus is one indicator of the strength of the TC secondary circulation (inflow at low levels, upward flow in the inner core, and outflow aloft). Additionally, synoptic-scale weather systems can induce divergence aloft in certain regions. If a TC moves into such a favorable region, its secondary circulation can be enhanced, contributing to intensification (Hendricks et al. 2010). Rappin et al. (2011) postulated that if divergence weakens in a region, subsidence may be forced that will act as an energetic drain on the TC.

The 200 mb divergence over Hurricane Joaquin was strong from 0000 UTC 3 October to 1800 UTC 3 October (Figure 17, orange line). Between 0000 UTC 4 October and 1200 UTC 4 October the divergence aloft weakens significantly, which correlates with some of the largest VWS magnitudes (Figure 17, blue line). The subsequent rapid decreases in VWS magnitudes leading up to 1800 UTC 4 October would normally be expected to have favored intensification.
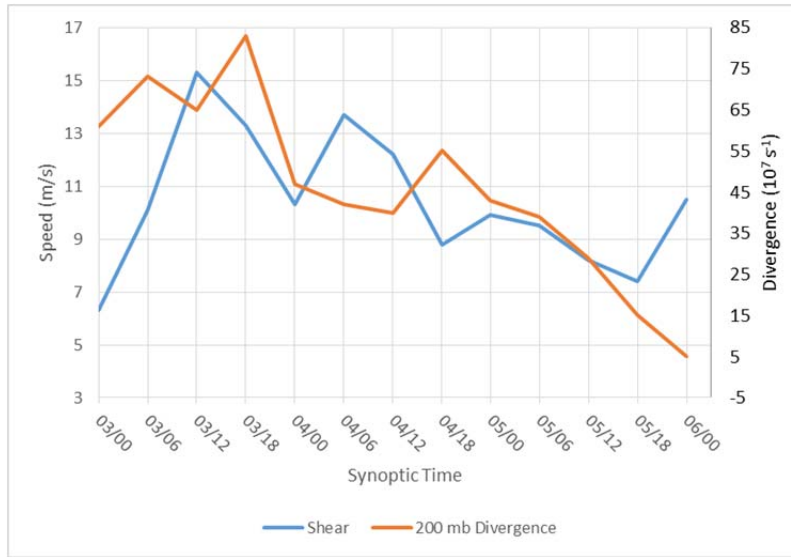
0-hour forecast showing 6-hourly shear (m/s, blue line) and divergence
(10^7s^{-1}, orange line) at 200 mb. Source: DeMaria et al. (2005).

Figure 17.   SHIPS Shear and 200 mb Divergence

Since 1800 UTC 4 October was the time of the interruption of the rapid
decay of Joaquin, and was also the time of increased 200 mb divergence (Figure
17, orange line), it is hypothesized that the dramatic decrease in VWS was a
prime environmental factor in the interrupted rapid decay of Joaquin. After 1800
UTC 4 October, the VWS magnitude was in the lower moderate VWS range
between 4 and 7 m/s, which recent studies (Reasor et al. 2004; Rios-Berrios and
Torn 2017) suggest may not be too inhibiting to TC formation and intensification.
Although the 200 mb divergence continues to weaken, this factor normally
associated with decreasing TC intensity may be balanced by a weakened VWS
magnitude and allow the intensity to remain constant from 0000 UTC 5 October
to 0000 UTC 6 October (Table 1). Although there were decreasing SSTs below
Joaquin between 0000 UTC 5 October and 0600 UTC 6 October, these SSTs
(~27°C) may have still provided the surface latent and sensible heat fluxes
needed to produce significant convection and low-level convergence.

Hendricks et al. (2010) correlated the mid-level relative humidity and TC intensity and found drier air made it more likely the TC was going to weaken. Hill and Lackmann (2009) stated that dry environments inhibit precipitation in the outer regions of a TC creating a decrease in the PV generation of the storm as a whole, while a relatively moist environment has the opposite impact. The mid-level relative humidity around Joaquin was relatively lower between 0000 UTC 3 October and 0600 UTC 3 October (Figure 18, blue line). However, the relative humidity then increased to between 60 and 70 % from 0000 UTC to 1800 UTC 4 October when Joaquin had decreasing intensities rather than increasing intensity as Hendricks et al. (2010) had found. Furthermore, the mid-level relative humidity subsequently steadily declined even though the intensity of Joaquin was constant rather than decreasing as the Hendricks et al. (2010) study would imply. Investigating the GFS 700 mb relative humidity (not shown) reveals a tongue of very dry air (10% relative humidity) south of Joaquin that makes an appearance at 1800 UTC 4 October. That area of low relative humidity persists until 0000 UTC 6 October and is wrapping into Joaquin throughout the time period. This provides strong evidence that the asymmetries in relative humidity should have continued to weaken Joaquin beyond 0000 UTC 5 October when in fact, they did not. Looking to the north of Joaquin reveals very moist air (at least 90% relative humidity) throughout the same time period.
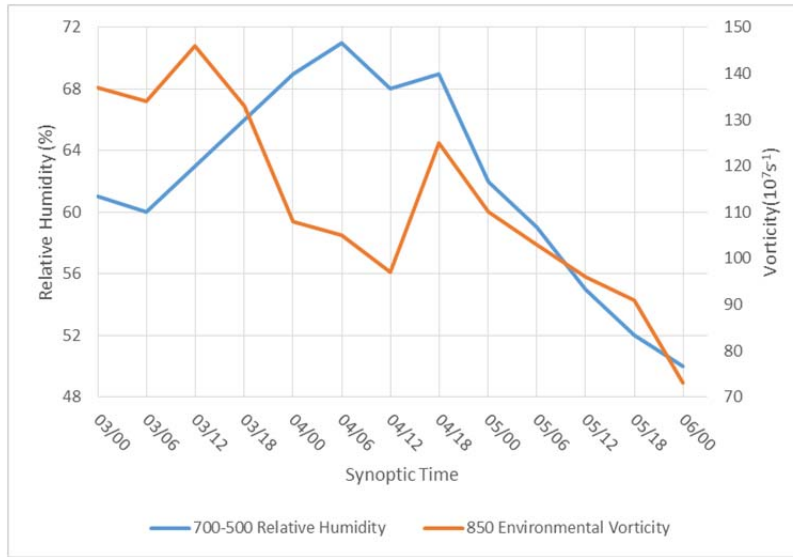
SHIPS 700-500 mb relative humidity (%, blue line) and 850 mb environmental vorticity ($10^7 s^{-1}$, orange line) Vorticity is multiplied by 10^7 to account for axis values. Source: DeMaria et al. (2005).

Figure 18.   SHIPS 700-500 mb Relative Humidity and 850 mb Environmental Vorticity

Gray (1968) had demonstrated that TC formation was favored in a region of environmental cyclonic vorticity (positive in the Northern Hemisphere). In this case, the 850 mb relative vorticity was large as Joaquin reached maximum intensity at 1800 UTC 30 October and was decreasing as Joaquin was rapidly decaying until 1200 UTC 4 October (Figure 18, orange line).The low-level vorticity then temporarily increased between 1200 and 1800 UTC 4 October, which is when the rapid decay was interrupted. Whether these 850 mb vorticity changes were causative or coincidental to the Joaquin intensity changes is not clear, as the vorticity then decreased while the intensity held constant for 30 hours.

In summary, periods of strong VWS, smaller low-level moisture content, and larger upper-level divergence in Joaquin during 3–6 October tend to have opposite tendencies from the rapidly intensifying (RI) and intensifying (I) cases in Hendricks et al. (2010).

By averaging the Atlantic Basin (ATL) relative humidity values for a neutral (N) tropical cyclone in Table 3, a baseline value for the relative humidity curve in Figure 18 can be established. During the interrupted decay phase, 0000 UTC 5 to 0000 UTC 6 October the relative humidity is plummeting, and is already significantly lower than the 63.6% typically expected for a tropical storm to maintain intensity. Hendricks et al. (2010) also calculated other average values of environmental factors near Atlantic TCs that were weakening (W), neutral (N), or intensifying (I) (Table 3). Using their average values for a (N) storm as the baseline for the 700-500 mb relative humidity between 0000 UTC 5 October and 0000 UTC 6 October led to significantly lower relative humidities than Hendricks et al. (2010) found were characteristic of a (N) storm. Thus, the mid-level relative humidity does not appear to have contributed to the interrupted rapid decay phase of Joaquin.

Table 3.   Average Values of Environmental Factors Near Tropical Cyclones
Source: Adapted from Hendricks et al. (2010)

Quantity	Basin	W	N	I
Deep-layer shear (m/s)	WPAC	12.09	10.64	9.87
	ATL	11.24	11.80	9.89
SST (°C)	WPAC	27.74	28.75	29.20
	ATL	28.23	27.96	28.58
850-mb relative humidity (%)	WPAC	77.83	78.75	80.01
	ATL	73.93	76.27	76.12
500-mb relative humidity (%)	WPAC	55.56	60.65	64.25
	ATL	48.83	50.98	52.43
850-mb divergence (10^{-6} s^{-1})	WPAC	21.99	21.79	21.95
	ATL	21.63	21.19	21.40
200-mb divergence (10^{-6} s^{-1})	WPAC	4.77	4.18	4.65
	ATL	4.61	3.02	3.37
$\partial\theta_E/\partial p$ (10^3 K Pa^{-1})	WPAC	0.15	0.16	0.20
	ATL	0.35	0.28	0.32
850-mb vorticity (10^{-6} s^{-1})	WPAC	14.13	13.02	13.04
	ATL	7.71	6.91	6.48

The most important quantities are relative humidity, the 200-mb divergence value and the 850-mb vorticity value for the Atlantic Basin only. Abbreviations are: weakening (W), neutral (N), intensifying (I).

The speed and direction of the storm (Figure 19) are a reflection of the environmental steering flow. The speed of the storm during the interrupted decay phase varies from approximately 5.8 m/s from 0000 UTC 5 October to 1200 UTC 5 October to approximately 7.2 m/s from 1200 UTC 5 October to 0000 UTC 6 October. The slowdown in storm speed coupled with a shift in the direction of motion of the storm from 55 degrees to 17 degrees prior to the interrupted rapid decay and then an increase in the storm speed and return to a heading of ~50 degrees indicate that the steering flow is first associated with the deep mid-latitude trough to the west and later by another trough farther north.

Storm speed (m/s, blue line) and direction (degrees, orange line) defined as a heading direction (degrees) relative to North toward which Joaquin is moving calculated from the NHC best-track.

Figure 19.   NHC Calculated Storm Speed and Direction

Vertical profiles of the zonal and meridional steering flow in the vicinity of Hurricane Joaquin from the ERA-Interim reanalysis dataset are shown in Figure 20. Prior to the interrupted decay period at 0000 UTC 4 October (Figure 20c) the 900-500 mb layer has almost uniform wind speeds of 9 m/s, which agrees well with the storm speed in Figure 19. Similarly, the 900-500 mb layer speed of ~5 m/s at the beginning of the interrupted decay at 0000 UTC 5 October agrees well

with the storm speed in Figure 19. Thus, the storm motion of Joaquin during this period is well correlated with the environmental steering flow (Elsberry et al. 2016).

Steering flow is defined by 900-500 mb layer flow, the red line is the zonal (U) flow, the blue line is the meridional (V) flow and the bold black line is the steering flow evolution. Courtesy of Elsberry et al. (2016).
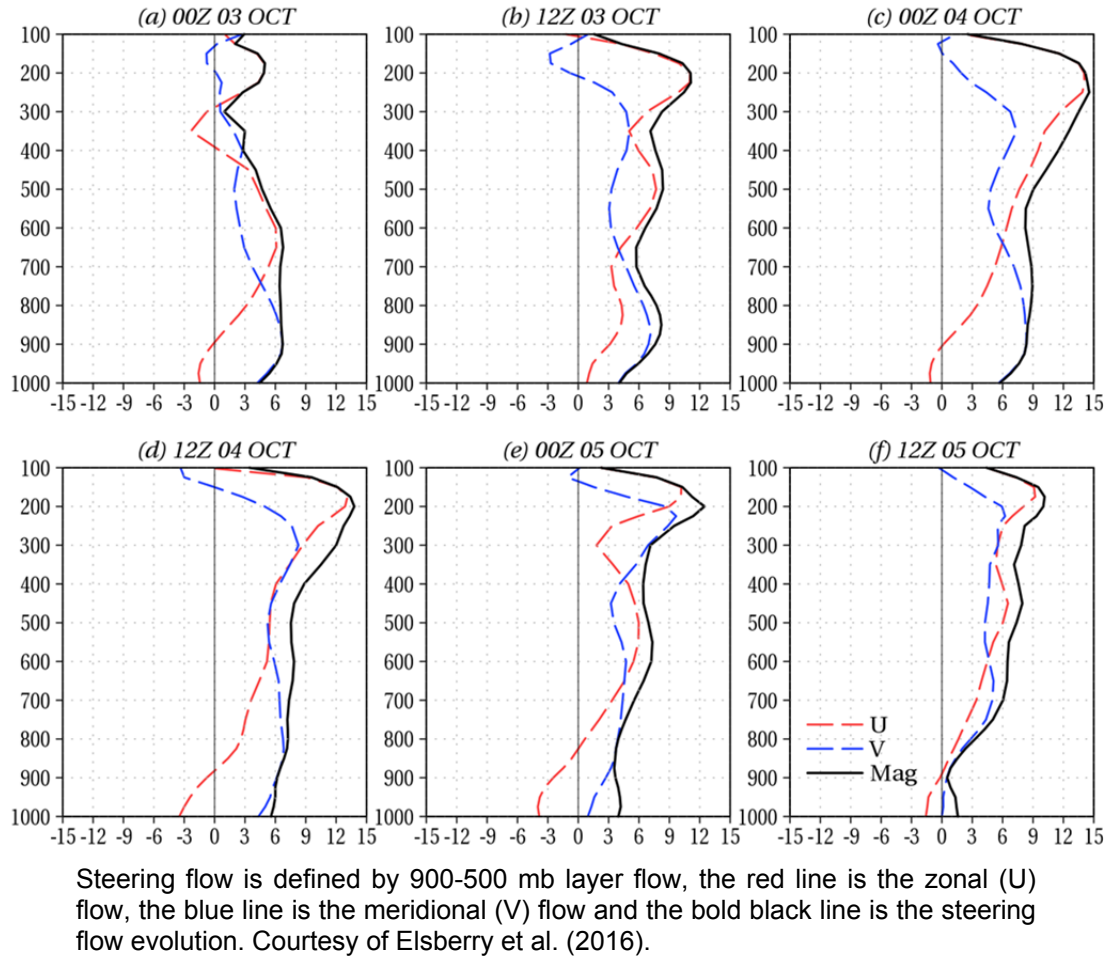
Figure 20.   Steering Flow Evolution for Hurricane Joaquin from 0000 UTC 3 October to 1200 UTC 5 October

These steering flow changes can be related to the synoptic scale circulations in the vicinity of Hurricane Joaquin. The mid-level wind evolution leading to the steering flow is displayed in the GFS analysis in Figure 21.
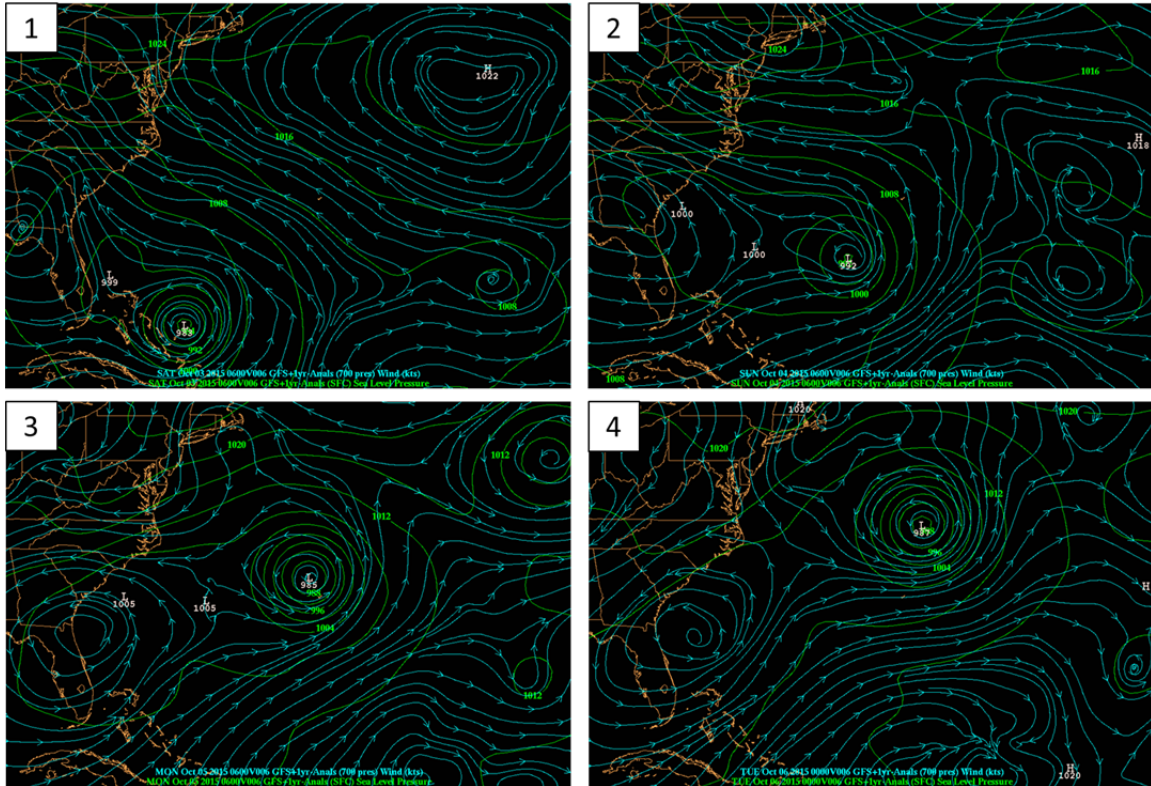
The evolution of mid-level (700 mb) winds as shown by GFS analyses for: (1) 0600 UTC 3 October, (2) 0600 UTC 4 October, (3) 0600 UTC 5 October and (4) 0000 UTC 6 October. The green lines represent MSLP and the blue streamlines represent 700 mb winds.

Figure 21.   Evolution of Steering Winds for Hurricane Joaquin

Joaquin is nearly stationary in the vicinity of the Bahamas as the streamlines show reasonable uniformity around the periphery of the storm (Figure 21, frame 1). In frame 2, Joaquin has begun to rapidly move to the northeast under the influence of southwesterly flow associated with the mid-latitude trough to the west and subsequent organization of the mid-level winds. In frame 3, Joaquin is moving slowly as the low center has moved out of the channel of southwesterly winds into a pocket of winds dominated by the circulation. Also noteworthy is the streamline that is being redirected on the northeast periphery of Joaquin into the high pressure center in the upper right hand corner. In frame 4, Joaquin continues to track northeastward and has begun to pick up speed due, in part, to the additional influence exerted by the

41

mid-level winds associated with the high pressure center located over Massachusetts.

B.   SPECIAL 15-MINUTE CIMSS VWS DATASETS

The CIMSS group also produced a special AMV dataset at 15-minute intervals for the entire lifecycle of Hurricane Joaquin, including the time period examined in this thesis. As described in Chapter III B. 4, the CIMSS group produces two VWS analyses with and without vortex removal. As stated in Park et al. (2012), the objective of calculating VWS is to average out the symmetric circulation and thus calculate a single wind vector at each level that is assumed to represent the uniform horizontal environmental flow. Thus, the CIMSS AMV algorithm has an option in which the vortex is removed and the VWS is calculated after averaging the winds from storm center out to specified radius. The radii chosen for this study are 350 km and 500 km. Averaging based on the former radius will retain environmental VWS closer to the TC while averaging based on the latter radius will retain environmental VWS farther away. The alternate CIMSS method, with the TC vortex not removed (VNR) is shown in the bottom two panels where the vortex is left in place and an annulus is utilized in an attempt to remove the storm winds from the VWS calculations. Similarly, two different annuli were chosen for the same reasons: inner and outer radii of 200 km and 500 km, respectively, and inner and outer radii of 200 km and 800 km, respectively.

The 15-minute AMV VWS with radii of 350 km and 500 km, and annuli of 200–500 km and 200–800 km, are compared in Figure 22. Good agreement is found between both the direction and magnitude of the VWS for the VR 0–350 km (Figure 22, top left) and VR 0–500 km (Figure 22, top right) calculations.
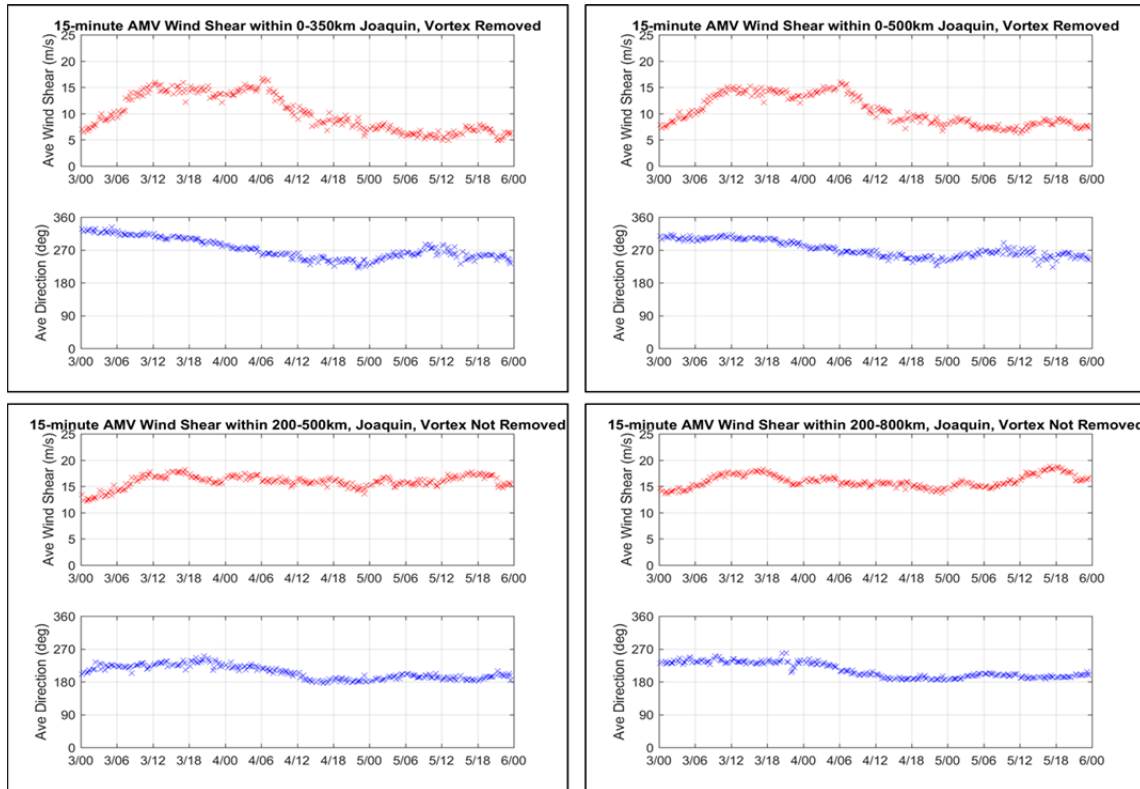
Time series of CIMSS VWS magnitude (m/s, red line) and direction (degrees, blue line) from which the VWS vector is coming [opposite of previous vector heading] from special set of 15-minute temporal resolution AMVs from 0000 UTC 3 October to 0000 UTC 6 October. The top left panel is calculated with the vortex removed and with an averaging radius of 350 km. The top right panel is calculated with the vortex removed and a radius of 500 km. The bottom left panel is calculated with the vortex not removed and an annulus from 200–500 km. The bottom right panel is calculated with the vortex not removed and an annulus from 200–800 km.

Figure 22.   15-minute AMV Wind Shear Comparison

Thus, not much sensitivity to the averaging radius is found when the vortex is removed and an averaging radius is less than 500 km. In both of these calculations with the vortex removed, the VWS magnitude averaged more than 15 m/s before 0600 UTC 4 October, which is during the period of rapid decay (Figure 14). However, a significant reduction in the average VWS magnitude begins shortly after 0600 UTC 4 October and by around 0000 UTC 5 October the VWS magnitude is reduced to a more moderate 8 m/s. It is noteworthy that it is during the period of moderate VWS that the interruption of the rapid decay of Hurricane Joaquin occurred, and the intensity was constant from 0000 UTC 5

October to 0000 UTC 6 October (Figure 14). These observations in Hurricane Joaquin are corroborated by the numerical simulation with 5 m/s VWS conducted by Frank and Ritchie (2001), who had numerically simulated a similar event of near-constant intensity after reduction of the VWS to a moderate VWS.

By contrast, the CIMSS VWS magnitude in which the vortex has not been removed (Figure 22, lower panels) continues to be very large (~15 m/s) throughout the period of interrupted rapid decay. Therefore, one would expect the rapid decay of Joaquin to have continued rather than have a period of constant intensity (Figure 14). However, the VWS directions from the calculation with the vortex not removed appear to be more closely aligned with the typical downshear alignment of a TC. Note that the VWS directions with the vortex not removed are from the west-southwest and then become more southerly during the period of interrupted rapid decay, which is consistent with the storm motion changes in Figure 19. By contrast, the VWS directions with the vortex removed begin with west-northwest directions and only gradually change to vectors from the west-southwest. In summary, the CIMSS VWS calculations based on a special AMV dataset with 15-minute frequency appear to be useful in revealing trends. However, more study is required as to the impacts of removing or not removing the vortex and of the area average versus the annulus approach for calculating the VWS.

The average VWS decreases rapidly after 0600 UTC 4 October, weakening from approximately 15 m/s to a relatively constant 8 m/s from 1500 UTC 4 October to 0000 UTC 6 October for the period immediately prior to the interrupted decay period (Figure 23). The shear simulations performed by Frank and Ritchie (2001) showed that weakening is not immediate in storms with VWS between 5 and 10 m/s which correlates nicely with the onset of the interrupted rapid decay period at 0000 UTC 5 October. Since the outflow of Joaquin can be considered to be a vortex-scale process and not related to the large-scale environment, the VR calculation is likely producing a more accurate representation of the deep layer VWS Joaquin was experiencing. This analysis

illustrates that caution should be taken when using a VWS value, averaged either vertically or horizontally as will be discussed below.

15-minute AMV Wind Shear within 0-500km Joaquin, Vortex Removed
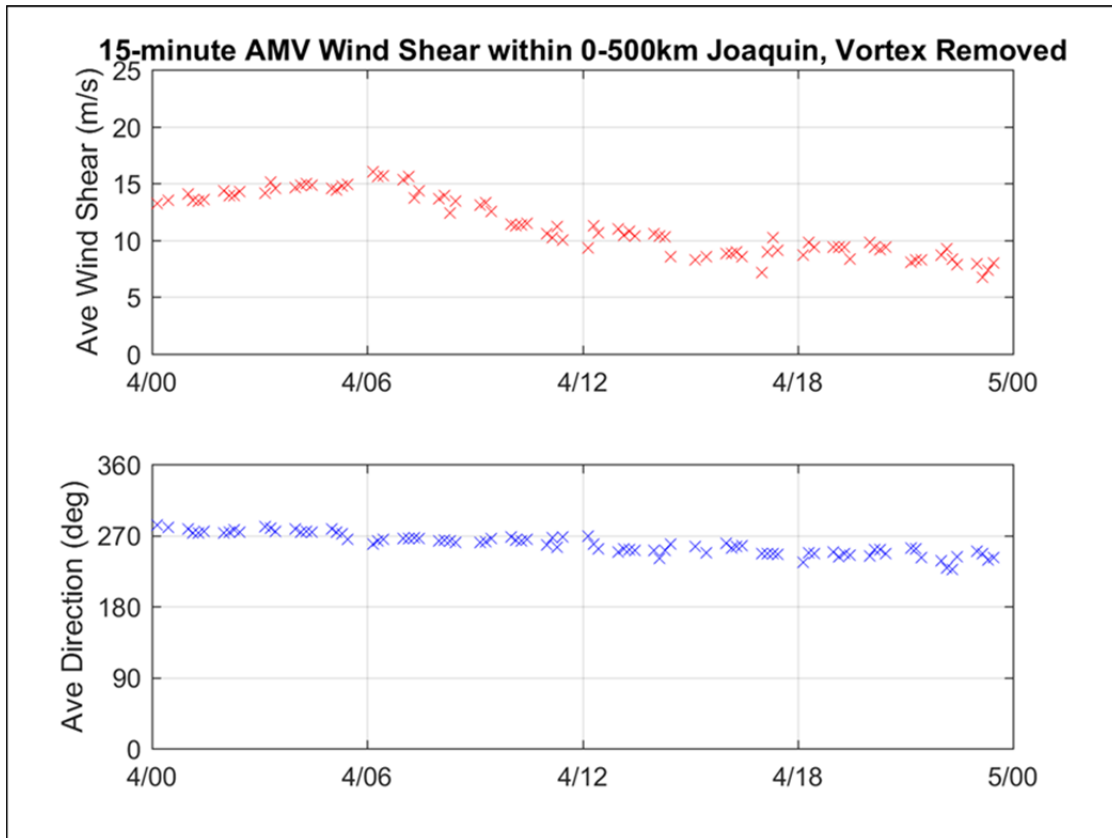
Truncated time series of 15 minute AMVs from 0000 UTC 4 October to 0000 UTC 5 October. The magnitude (m/s, red 'x') and direction (degrees, blue 'x') is calculated with the vortex removed and radius of 500 km.

Figure 23. 15-minute AMV Wind Shear before
Interrupted Rapid Decay Period

Depicting the horizontal plan views of the VWS in the immediate vicinity of Joaquin provides a wider lens for the investigation of the relationship of VWS and intensity change. Joaquin has settled into weaker VWS and the translation speed has slowed dramatically (Figure 24). Since the SST in the area of Joaquin is approximately 28°C, this SST is still in the range of temperatures conducive to TC intensification as postulated by Nyoumura and Yamashita (1984).

45
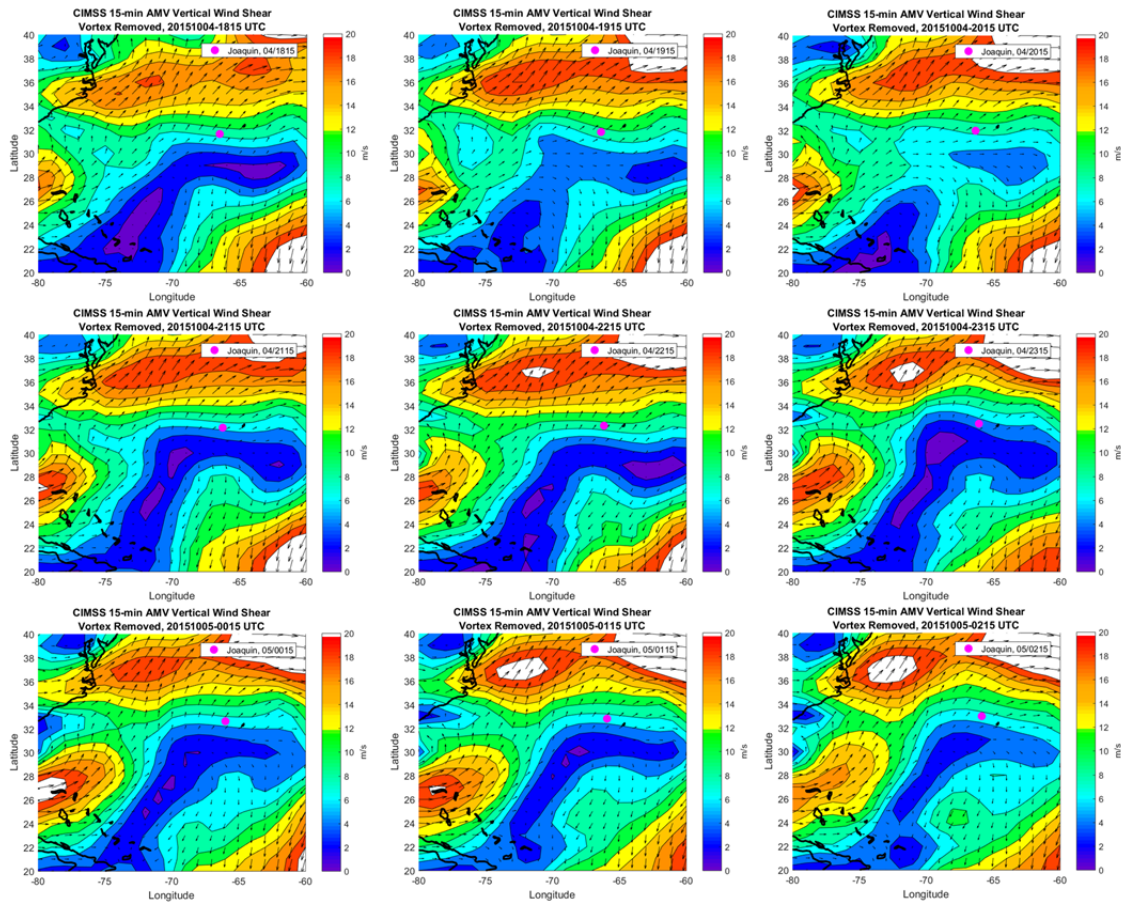
Hurricane Joaquin depicted in the CIMSS calculated vortex removed VWS fields hourly from 1815 UTC 4 October to 0215 UTC 5 October after the onset of weakened VWS but prior to the period of constant intensity. Field displays wind shear less than 20 m/s.

Figure 24.   Vortex Removed VWS Field Immediately Preceding and Following Onset of Interrupted Decay

The CIMSS VWSs in which the vortex has not been removed is shown in Figure 25. The area of VWS greater than 20 m/s is significantly larger and four degrees of latitude farther south than in the VR VWS panel in Figure 24. At this time, Joaquin is located in an area of VWS of approximately 10 m/s.

However, the VWS vectors appear to be associated with the vortex circulation (Figure 26). Note that the VWS vectors that appear to spiral out from the center (Figure 25) appear to be related to Joaquin's outflow (Figure 26) rather than the environment. The area of low VWS between 75ºW and 70ºW is being

supplanted by the area of stronger VWS to the west as the panel steps through the entire time period.
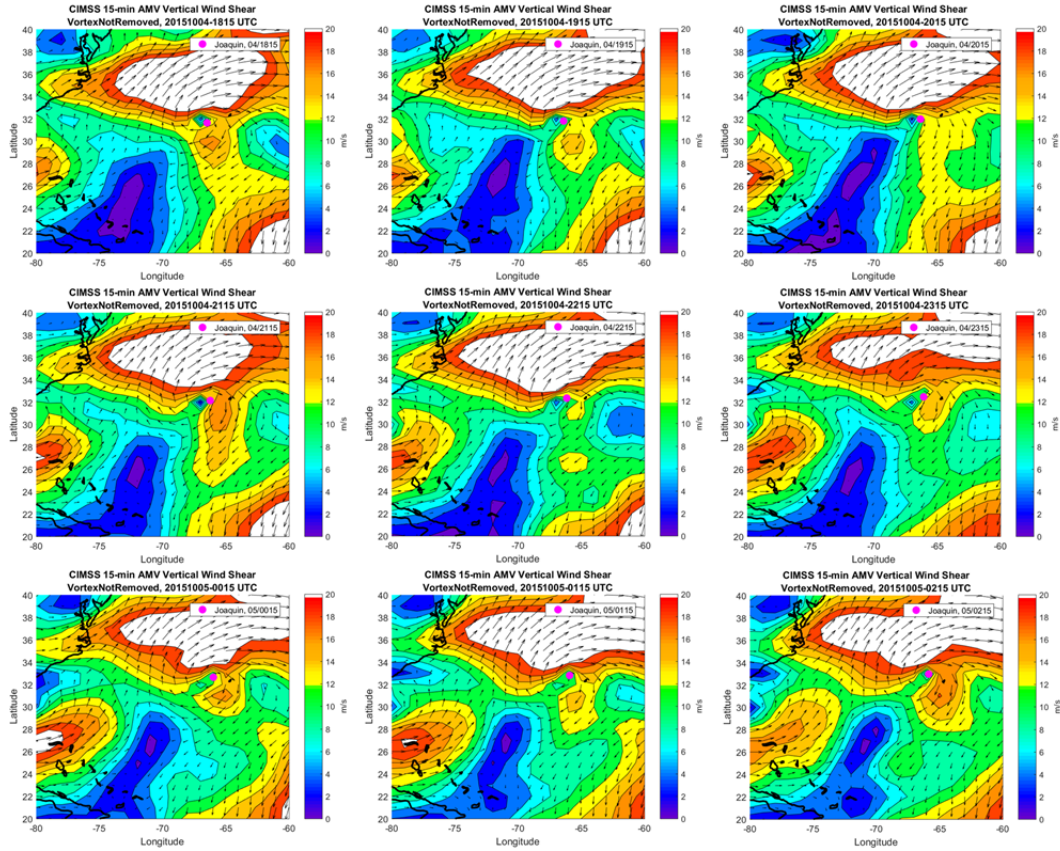

Hurricane Joaquin depicted in the CIMSS calculated vortex not removed shear field from 1815 UTC 4 October to 0215 UTC 5 October after the onset of weakened VWS but prior to the period of constant intensity. Field displays wind shear less than 20 m/s.

Figure 25.   Vortex Not Removed VWS Field Immediately Preceding and Following Onset of Interrupted Decay
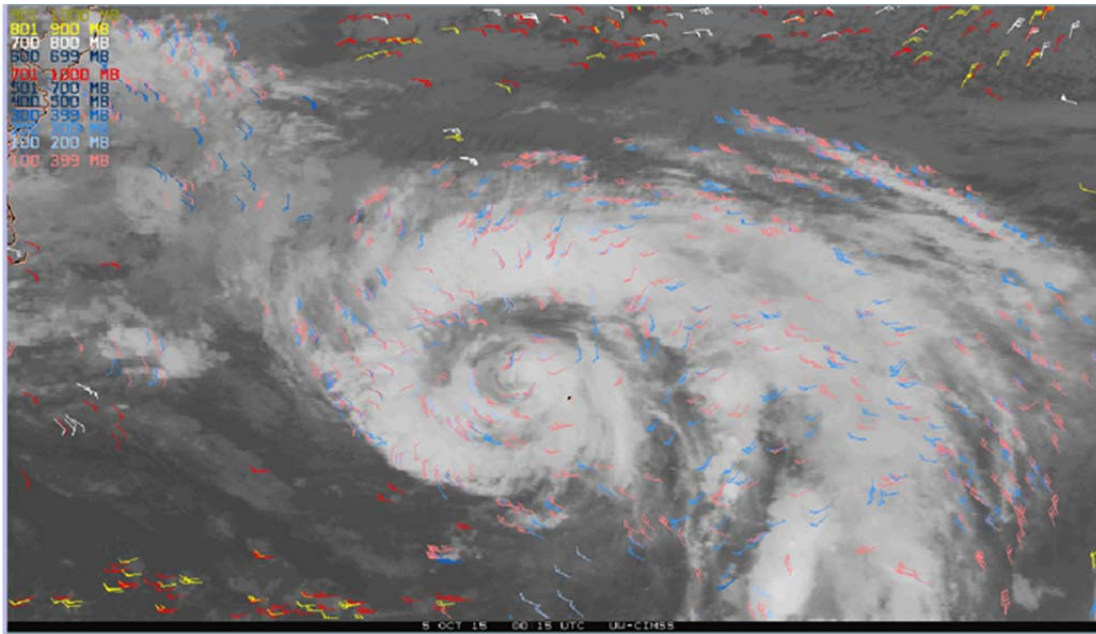
0015 UTC 5 October AMVs. Pink wind barbs indicate 100–399 mb average magnitude and direction. Red wind barbs indicate 701-1000 mb average magnitude and direction. Courtesy of Chris Velden, UW-CIMSS.

Figure 26.   0015 UTC 5 October AMVs

The area of VWS greater than 20 m/s north of Joaquin has extended westward in each of the panels in Figure 25. The area of weak shear southwest of Joaquin has been significantly altered from both east and west as areas of larger VWS have begun to converge. Joaquin is still in an area of VWS that averages approximately 10 m/s, still significantly larger than in the vortex removed panel.

C.   SYNTHESIS

In summary, most of the environmental factors discussed above cannot be used to explain the interrupted rapid decay of Joaquin. Indeed, these environmental factors would indicate Joaquin should have continued to weaken beyond 0000 UTC 5 October. For example, the SST is not high enough to contribute to Joaquin remaining even a neutral TC (Nyoumura and Yamashita (1984; Hendricks et al. 2010). The decreasing divergence aloft also would suggest a continuing decay of Joaquin. Low relative humidity in the mid-levels

seems to imply a significant ingestion of dry air into Joaquin, which again should lead to further weakening. The environmental vorticity is large enough that there should be a physical expansion of the storm, which is another factor that should contribute to Joaquin continuing to weaken. Even the northeastward storm direction should be contributing to the decay of Joaquin as it moves over lower SSTs.

The special AMV dataset at 15-minute intervals provides an environmental VWS picture that may explain the interrupted rapid decay that occurred in the later stages of Hurricane Joaquin. The 15-minute AMV wind fields provide high temporal resolution VWS magnitudes and directions that reveal trends that may not be evident in the typical 6-hourly frequency. In both of the CIMSS VWS calculations with the vortex removed, the VWS magnitude decreased from more than 15 m/s during the period of rapid decay to a more moderate (8 m/s) VWS at the time of interrupted rapid decay of Hurricane Joaquin and maintenance of a constant intensity for about 30 hours. By contrast, the CIMSS VWS calculation in which the vortex was not removed continued to have the very large VWS magnitudes, and this could not be used to explain the interrupted rapid decay of Hurricane Joaquin. However, this version of the CIMSS VWS with the vortex not removed appeared to have circulations that agreed better with the storm alignment changes in time. The average VNR shear values (Figure 22, bottom panels) correlate more closely with the alignment of the storm than the average VR shear values (Figure 22, top panels). A weakening of the VWS combined with a slower translation speed may have aided the interrupted rapid decay as the storm might have had time to re-align itself in a more vertical position. The main conclusion is that the weakening of the VWS was significant enough to cause the interrupted decay of Joaquin, even though all other environmental factors were negative. In the next chapter, vortex interaction with VWS using TCI-15 datasets will be investigated to understand possible internal factors that may have contributed to Joaquin maintaining intensity in a moderate VWS environment when most of the other factors were unfavorable.

THIS PAGE INTENTIONALLY LEFT BLANK

V.   INTERNAL FACTORS AFFECTING TC INTENSITY

Having examined the environmental factors contributing to the interrupted decay of Hurricane Joaquin, this chapter focuses on the response of the vortex to environmental VWS. First the evolution of the vortex tilt is examined using the ZWC tool. Then the analysis of the surface wind field is conducted to understand the response of the low level winds to the environmental VWS.

A.   VORTEX TILT

The first and most important factor when investigating the internal factors that may have contributed to the interrupted rapid decay of Hurricane Joaquin is the tilt of the vortex. Vortex tilt is the change in vertical position of the center from top to bottom under the influence of VWS (Reasor et al. 2004). In particular, a characteristic of a vortex being disrupted by VWS is a large vertical tilt, while a characteristic of a vortex that is resisting VWS is a lesser tilt.

Collecting the pertinent data for comparing ZWC tilt and the calculated VWS is crucial to drawing conclusions on the role played by VWS in the deformation of Joaquin (Table 4). Column 1 is the date of the ZWC calculation and the three heights at which the calculations were done. The minimum height is always 1500 meters, but the maximum height is either 10,500 meters or 14,500 meters dependent on the maximum elevation at which HDSS wind direction changes from the WB-57 mission can be used to infer a ZWC. The height that delineates the upper level from the lower level was arbitrarily chosen where the unsteady movement of the upper layer significantly changed providing an opportunity to show tilt and azimuth differences (Creasey, personal communication). Columns 2 and 3 show the course in degrees and speed in m/s of the storm at the synoptic times listed in column 1. Columns 4 and 5 show the vertical tilt of the vortex in degrees and in km. The vertical tilt in degrees is the angle between the higher level center and a vertical axis through the low level center. The vertical tilt in km is the distance calculated from storm center at a

lower level to the storm center at a higher level, and defined mathematically by the tangent of the tilt angle multiplied by vertical distance between the higher and lower level centers. For example, the vertical tilt in km from 1,500 m to 14,500 m is the distance the 14,500 m center is displaced from the 1,500 m center. Column 6 shows the azimuthal direction of the vortex tilt in degrees, where 0 degrees is north. Columns 7 and 8 show the CIMSS 6-hourly deep-layer VWS magnitude in m/s and direction in degrees. Columns 9 and 10 show the SHIPS 6-hourly deep-layer VWS magnitude in m/s and direction in degrees.

Table 4.   ZWC Vortex tilt, CIMSS 6-hourly and 15-minute VWS,
and SHIPS 6-hourly VWS

ZWC						CIMSS 6-hourly VWS		SHIPS 6-hourly	
	Storm Course (deg)	Storm Speed (m/s)	Vertical-Tilt (deg)	Vertical-Tilt (km)	Dir-Azimuth (deg)	Shear Direction (deg)	Magnitude (m/s)	Shear Direction (deg)	Magnitude (m/s)
1800 UTC 2 October	26	3.45				191	6.0	151	4.9
1500 - 10500 meters			52	11.5	335				
1500 - 6500 meters			35	3.5	310				
6500 - 10500 meters			66	9	346				
1800 UTC 3 October	57	8.75				110	18.6	127	13.2
1500 - 14500 meters			45	13	199				
1500 - 9500 meters			9	1.2	90				
9500 - 14500 meters			70	13.7	204				
1800 UTC 4 October	23	4.6				54	13.3	66	4.9
1500 - 10500 meters			61	16.2	102				
1500 - 5500 meters			43	3.7	53				
5500 - 10500 meters			71	14.5	112				
1800 UTC 4 October	23	4.6				54	13.3	66	4.9
1500 - 10500 meters			77	39	49				
1500 - 5500 meters			20	1.4	00				
5500 - 10500 meters			81	31.6	51				
1800 UTC 5 October	64	12.3							
1500 - 14500 meters			54	17.9	138	74	8.4	39	3.9
1500 - 9500 meters			30	4.6	15				
9500 - 14500 meters			77	21.7	149				

ZWC vortex tilt values in degrees and km, CIMSS 6-hourly VWS analyses and SHIPS 6-hourly VWS analyses. All directions are in degrees and all speeds are in m/s. Table compiled from Creasey, personal communication.

As explained in Creasey and Elsberry (2017), calculating the tilt of the vortex requires a minimum of three sondes be dropped within the eye region. Vertical differences are then calculated over 1-km layers to define an average

wind vector. A first guess of storm translation speed and direction is required to place the sonde in the correct storm relative horizontal and vertical positions. Then the HIRAD swath is used to create a surface wind isotach analysis and a geometric zero-isotach position approximates the ZWC within the eye. A second overpass of the storm center will provide additional information to refine the ZWC two positions by using the translation speeds in the storm-relative calculation. That is, the two ZWC estimates can be used to converge on storm translation speed and direction by dividing the distance between the two ZWC estimates by the time interval between overflights of the TC center.

The vortex tilt based on the dropsonde data from two overpasses of the storm on 2 October displays a remarkable vertical stacking of the vortex (Figure 27). Over the vertical extent of Joaquin (1500-10500 meters), the vortex tilt is only 11.5 km, and almost all of the tilt is in the 6500–10500 meter layer. This upper-layer tilt may simply indicate a wobble in the vortex (Creasey, personal communication). Joaquin had a MSLP of 941 mb and maximum sustained winds of 110 kts (Berg 2016) and was under the influence of deep-layer shear between 4.9 (SHIPS) and 6 (CIMSS) m/s from the northwest (SHIPS) or almost directly from the north (CIMSS) (Table 4). The 15-min VWS plot for this time (not shown) indicates Joaquin's center was located in an area of almost no VWS, which is consistent with the vortex tilt of only 11.5 km from the HDSS observations. This is a baseline ZWC plot as 2 October was prior to the rapid decay and subsequent interruption of that decay.
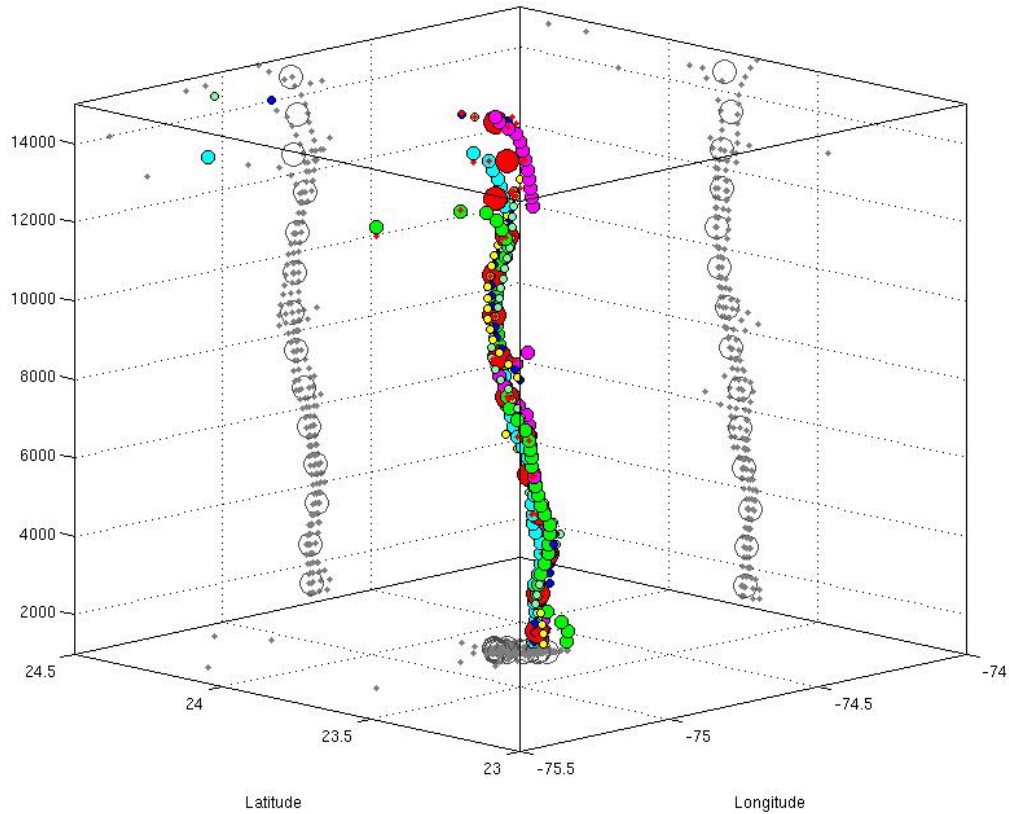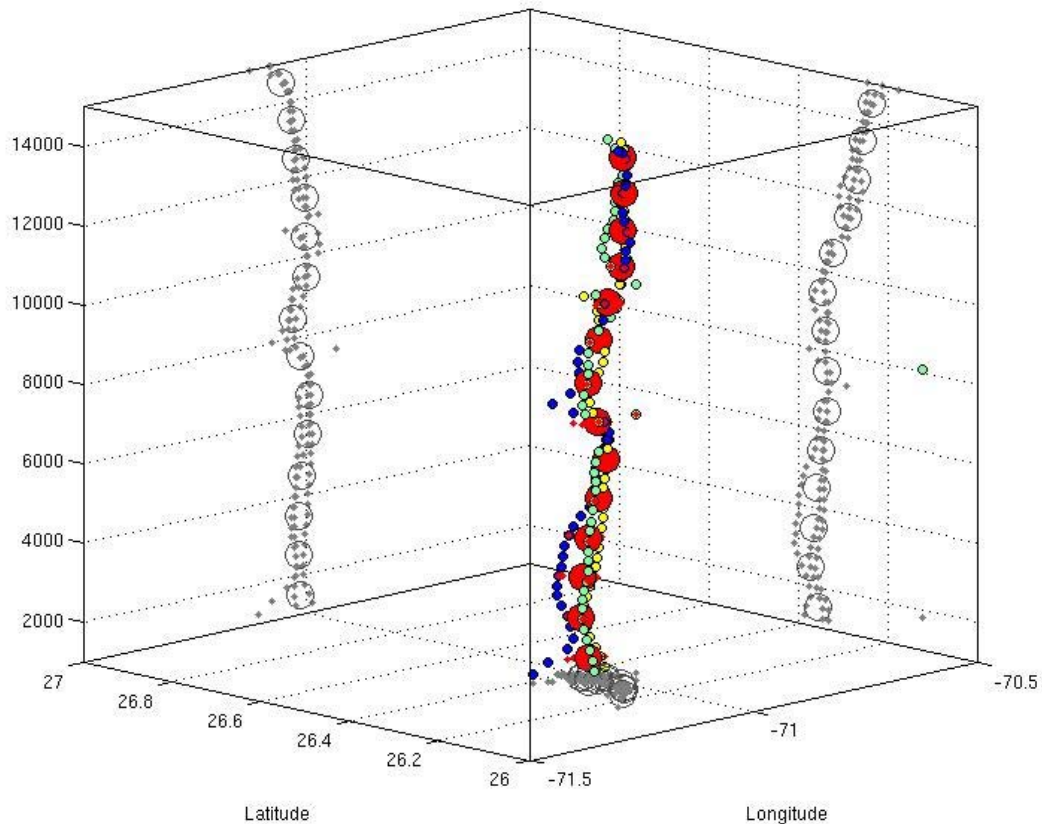
Vortex tilt between vertical heights of 1 km and 10 km in storm-relative coordinates from pass 1 and pass 2 over Hurricane Joaquin around 1800 UTC 2 October derived from HDSS sonde average wind directions over 1-km layers (large red circles) and at intermediate 200-m intervals (small colored circles). (Courtesy of Creasey 2017) CIMSS 6-hourly VWS is 191 at 6 m/s and SHIPS 6-hourly VWS is 151 at 4.9 m/s.

Figure 27.   Zero Wind Center Vortex Tilt for Hurricane Joaquin at 1800 UTC 2 October

The vortex tilt at 1800 UTC 3 October using only the first overpass by the NASA WB-57 aircraft has begun to tilt to the southwest (Figure 28). Over the vertical extent of Joaquin (1500–14500 meters) the vortex is again vertically stacked with a vortex tilt of only 13.6 km from the south-southwest concentrated in the 9500–14500 m layer. Joaquin had reached peak intensity of 135 kt around 1200 UTC 3 October and at 1800 UTC 3 October Joaquin had a MSLP of

934 mb and maximum sustained winds of 130 kt (Berg 2016). Both the SHIPS VWS of 13.2 m/s and CIMSS VWS of 13.6 m/s toward the southeast indicate that a decrease in intensity is to be expected and indeed Joaquin had begun to decay rapidly (Table 1).

Vortex tilt between vertical heights of 1.5 km and 14.5 km in storm-relative coordinates from pass 1 over Hurricane Joaquin around 1800 UTC 3 October derived from HDSS sonde average wind directions over 1-km layers (large red circles) and at intermediate 200-m intervals(small colored circles). Courtesy of Creasey, 2017. CIMSS 6-hourly VWS is 110 at 18.6 m/s and SHIPS 6-hourly VWS is 127 at 13.2 m/s.

Figure 28.   Zero Wind Center Vortex Tilt for Hurricane Joaquin at 1800 UTC 3 October

The vortex of Joaquin had a significant increase in the east-west tilt by 1800 UTC 4 October (Figure 29, top). While the north-south tilt is only 16 km, the east-west tilt is 39 km. Thus, the vortex is azimuthally oriented toward the east-southeast (102 degrees, Table 4). Another very marked change is that the upper layer of the ZWC plot (4500–10500 meters) has rotated cyclonically from 112 degrees to 51 degrees in one hour (Figure 29, bottom) (Creasey, personal communication). The rapid decay has been occurring over the last 24 hours as Joaquin has filled by 25 mb to a MSLP of 958 mb and wind speeds have dropped by 45 kt to a maximum of 85 kt. The deep-layer VWS from SHIPS of only 4.6 m/s is not consistent with the large vortex tilt of 39 km, but the CIMSS deep-layer VWS of 13.2 m/s is consistent with the large vortex tilt.

The 1500–14500 tilt of the vortex was reduced from 39 km at 1800 UTC 4 October to 17.9 km at 1800 UTC 5 October, but there is almost no tilt (4.6 km) in the lowest 8.5 km (Figure 30). As this deep-layer vortex tilt is azimuthally oriented toward the northeast, Joaquin at this time has a TC-like structure below 8.5 km with an outflow that is streaming to the northeast in response to a mid-latitude trough to the northwest. This decrease in the low- to mid-tropospheric vortex tilt may be attributed to the decrease in the CIMSS VWS from 13.2 m/s at 1800 UTC 4 October to a more moderate value of 8.4 m/s at 1800 UTC 5 October, or for the SHIPS VWS remaining around 4 m/s (Table 4) Hurricane Joaquin has filled by another 6 mb to a MSLP of 964 mb over the past 24 hours and wind speeds have dropped to a maximum of 75 kt (Table 1), which is reasonable for a vortex tilt structure as in Figure 30.
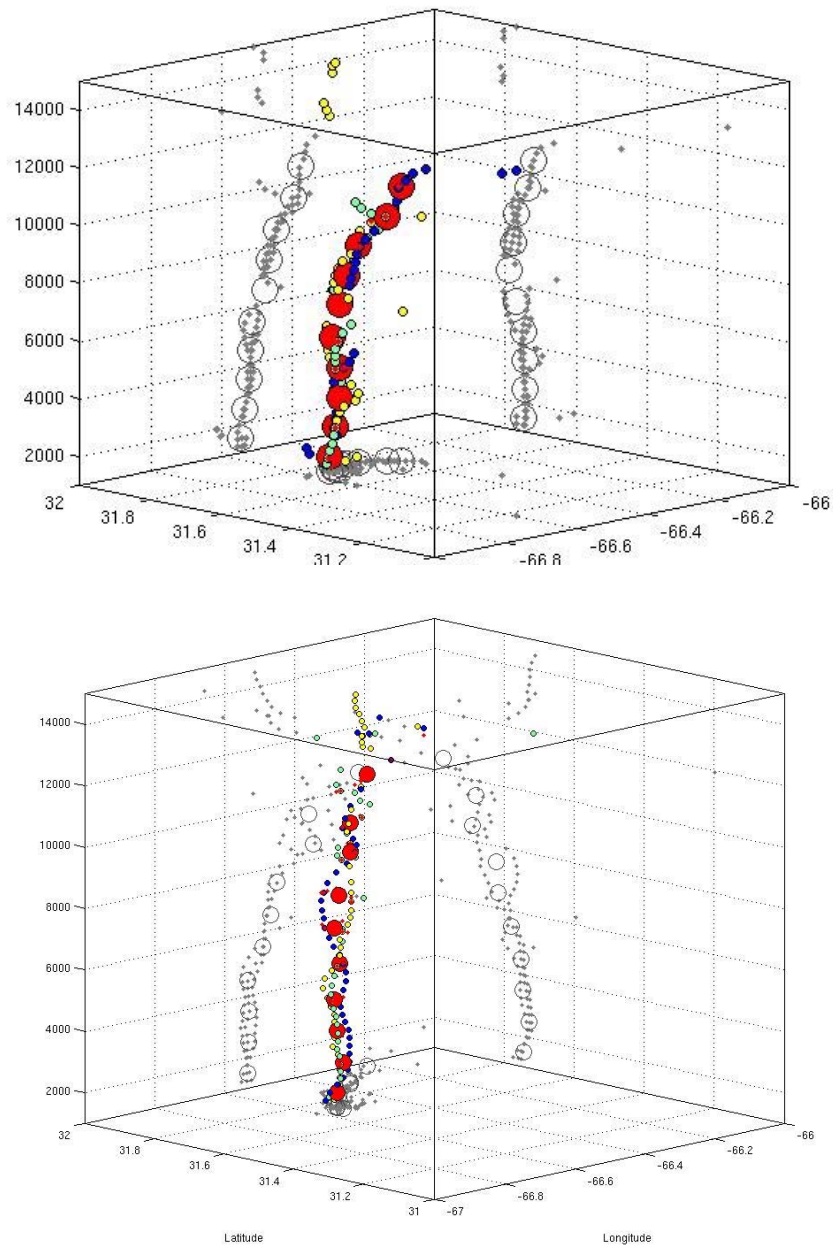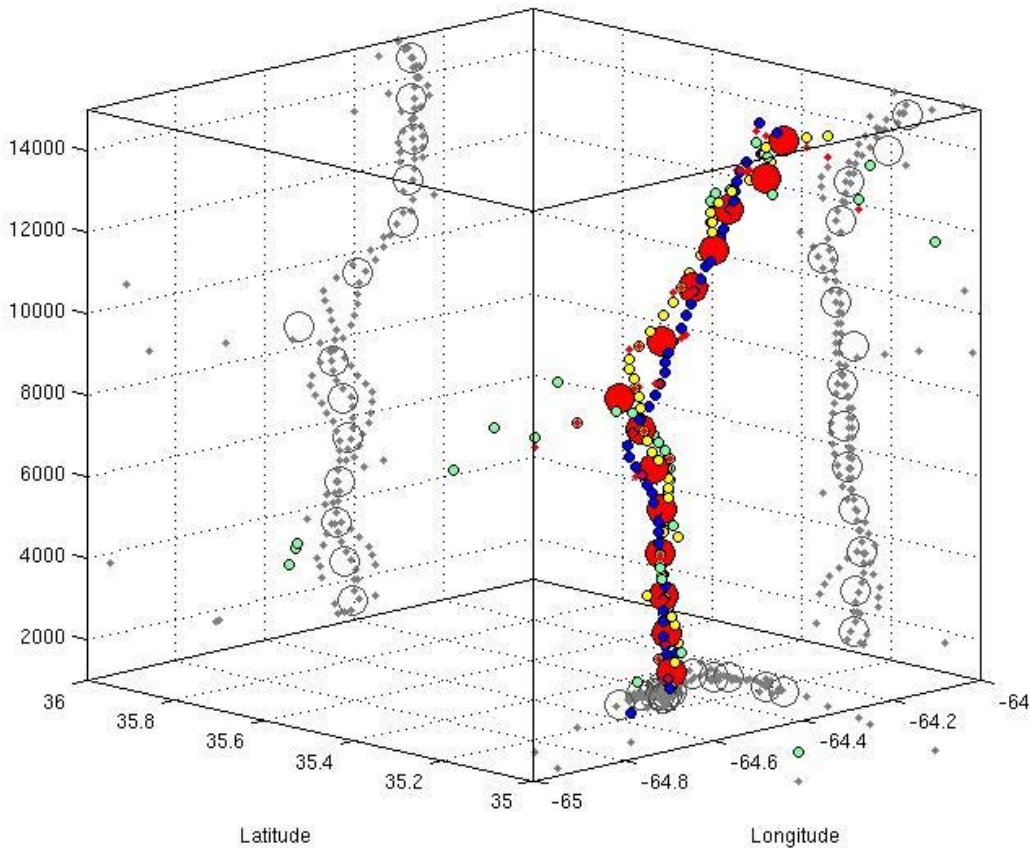
Vortex tilt between 1.5 km and 14.5 km in storm-relative coordinates from pass 1 (top panel) around 1800 UTC 4 October and pass 2 (bottom panel) around 1900 UTC 4 October over Hurricane Joaquin derived from HDSS sonde average wind directions over 1-km layers (large red circles) and at intermediate 200-m intervals(small colored circles). Courtesy of Creasey, 2017. CIMSS 6-hourly VWS is 54 at 13.3 m/s and SHIPS 6-hourly VWS is 66 at 4.9 m/s.

Figure 29.   Zero Wind Center Vortex Tilt for Hurricane Joaquin
                    at 1800 UTC 4 October

Vortex tilt between 1 and 10 km in storm-relative coordinates from pass 1 over Hurricane Joaquin around 1800 UTC 5 October derived from HDSS sonde average wind directions over 1-km layers (large red circles) and at intermediate 200-m intervals(small colored circles). Courtesy of Creasey, 2017. CIMSS 6-hourly VWS is 74 at 8.4 m/s and SHIPS 6-hourly VWS is 39 at 3.9 m/s.

Figure 30.   Zero Wind Center Vortex Tilt for Hurricane Joaquin
at 1800 UTC 5 October

These vortex tilt values are higher than the vortex tilt values calculated at 1800 UTC 3 October when Joaquin was experiencing the strongest VWS (Table 4). It must be noted that while Joaquin was experiencing the strongest VWS at 1800 UTC 3 October, it was also near its peak intensity which may have allowed it to resist the VWS for a period of time (indeed the vortex had a larger vertical extent as shown by ZWC tilt plots). Also, since the largest vortex tilt was in the upper layer of the ZWC calculation and Finocchio et al. (2016) concluded that

upper-level shear is more favorable for TC intensification because the boundary layer downwind of the convective complex (typically downshear left (Corbosiero and Molinari 2003; Reasor et al. 2004; DeHart et al. 2014)) stays relatively warm and moist.

In summary, the weakening of the VWS over a 24-hour period has allowed Hurricane Joaquin to become more vertically stacked in the lower to middle troposphere (tilt of 4.6 km)at 1800 UTC 5 October.

To understand the tilt of Joaquin, the idealized simulation by Frank and Ritchie (2001) should prove informative. The numerical simulation conducted by Frank and Ritchie (2001) began with idealized initial conditions including using 20 vertical levels, 50 mb as the top of the model, performing the simulations on an *f*-plane to limit interactions between the storm flow and the absolute planetary vorticity gradient. The *f*-plane helped ensure that the shear affecting the inner core is similar to that imposed over the entire region. None of the simulations performed included radiative processes. The SST was fixed at 28.5°C and all simulations began with the same baroclinic, axisymmetric vortex at a radius of 135 km. When large-scale wind fields are imposed (t = 48 h), they are zonal and uniform at each sigma level. Frank and Ritchie (2001) noted that if the VWS is around 5 m/s, a tilt of no greater than 3 km develops for the 850-500 mb or the 850-200 mb layers until approximately t = 96 h. The VWS causes this case to start to fill between 87-90 hours and then levels off at 965 mb at t = 111 h, maintaining that intensity through the end of the simulation (Figure 31). At the later simulation times, there is a correlation between the decreasing intensity of the storm and the increase in the tilt of the vortex. It stands to reason that the 5 m/s shear has overcome the internal processes of the TC to begin to tilt the vortex, which causes the subsequent drop in intensity. The only seeming anomalous behavior occurs at t = 114 h where both layers are exhibiting a tilt of approximately 7 km that indicates the two layers have become vertically stacked, which may account for the resultant small increase in intensity at that time. There

59

seems to be a correlation between the input of the VWS and the tilt of the vortex that closely mimics that of Joaquin.
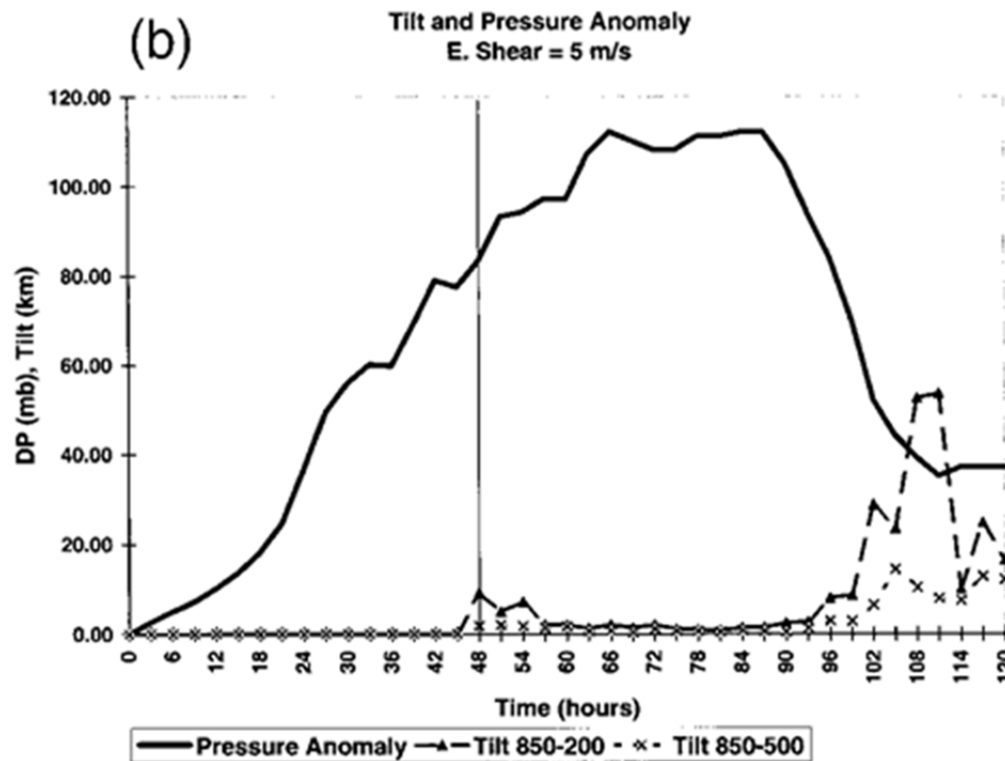
Time series of storm pressure anomaly and tilt of the simulated storm vortex between 850-200 mb and 850-500 mb with a constant 5 m/s VWS applied after t = 48 h. Altered from Frank and Ritchie (2001).

Figure 31.   Simulated Vortex Tilt under 5 m/s VWS

The first indication of a significant tilt in the vortex occurs at t = 102 h in the 850–200 mb layer and that occurs almost exclusively between 500–200 mb (Figure 32). Using Creasey and Elsberry's (2017) method for calculating zero wind centers (ZWC) and the tilt of the vortex was the opportunity to discover whether or not a correlation exists for the moderate VWS case of Joaquin and the simulated case performed by Frank and Ritchie (2001).
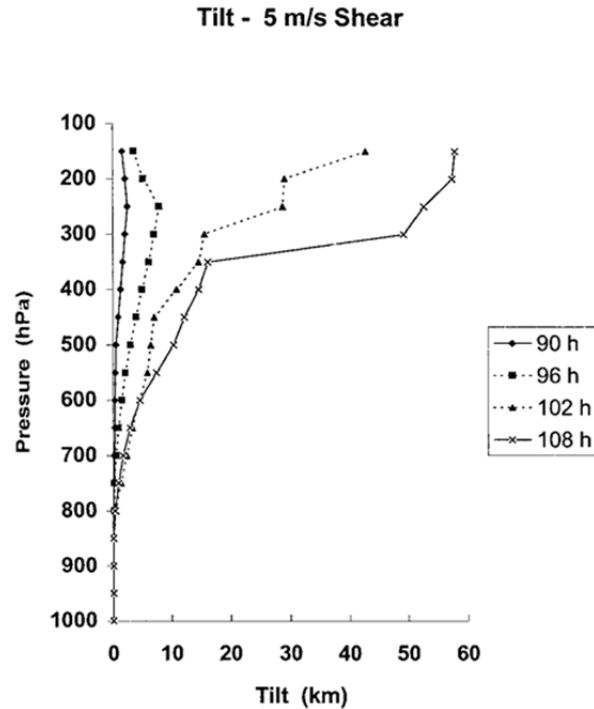
Tilt - 5 m/s Shear

Simulated vertical profiles of the axis tilt at 4 times in the 5 m/s shear case. Courtesy of Frank and Ritchie (2001).

Figure 32.   Vortex Tilt of Idealized TC Simulation under 5 m/s VWS

B.   SURFACE WIND ANALYSIS

In addition to investigating the potential impacts that VWS in the mid- to upper- levels had on the evolution of Hurricane Joaquin, it is instructive to explore the evolution of the surface wind field. Using the Regional and Mesoscale Meteorology Branch (RAMMB) of the Cooperative Institute for Research in the Atmosphere (CIRA) aircraft-based TC surface wind analyses for Hurricane Joaquin will provide 6-hourly surface wind fields compiled from numerous sources of data.

The deformation of the wind field at the surface with the most axisymmetric structure is illustrated at 0000 UTC 3 October (Figure 33, top left). In the top right panel (0600 UTC 3 October), the 80 kt contour has been deformed from an ellipsoid isotach to an enclosed isotach on the southern periphery of the eyewall region. The 64 kt radius has remained essentially

61

unchanged from the top left panel. The 50 kt radius has decreased in size in all four quadrants. The 34 kt radius has decreased in the southeast and southwest quadrants while it has increased significantly in the northwest quadrant as the analysis includes the spiral band that has continued to develop as in the top left panel.
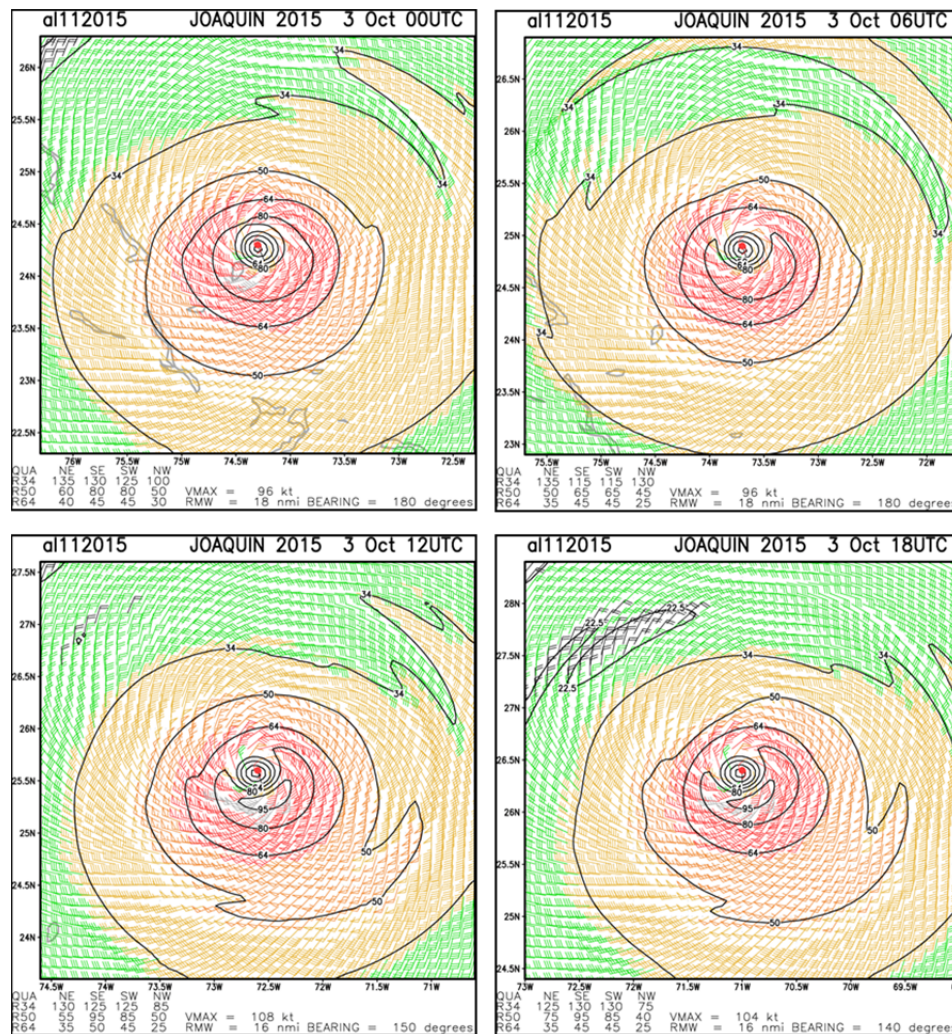
RAMMB compiled surface wind analysis for Hurricane Joaquin at synoptic times. 0000 UTC 3 October (top left) VWS is 166 at 6.6 m/s (CIMSS) and 134 at 5.3 m/s (SHIPS), 0600 UTC 3 October (top right) VWS is 140 at 10.4 m/s (CIMSS) and 131 at 10.7 m/s (SHIPS), 1200 UTC 3 October (bottom left) VWS is 130 at 17.5 m/s (CIMSS) and 132 at 13.1 m/s (SHIPS), and 1800 UTC 3 October (bottom right) VWS is 110 at 18.6 m/s (CIMSS) and 127 at 13.2 m/s (SHIPS). Wind speed is measured in knots and direction of VWS is degrees. Source: RAMMB Archive.

Figure 33.   Surface Wind Field for Hurricane Joaquin 3 October

The bottom left panel (1200 UTC 3 October) is the time when Joaquin reaches maximum intensity. Note that a tightened gradient has produced a 95 kt isotach that roughly mimics the shape of the 80 kt isotach. The 80 kt isotach has shifted from the southern periphery of the eyewall region to the south-eastern periphery. The 64 kt radius has remained essentially unchanged. The SHIPS VWS has increased between 0000 UTC and 1200 UTC 3 October to a value of 13.1 m/s out of the northwest which correlates nicely with the deformation forming in the northwest quadrant of Joaquin and the subsequent expansion of wind radii in the southeast quadrant. The 34 kt radius has returned to a similar size as in the 0000 UTC analysis.

In the bottom right panel (1800 UTC 3 October) there is very little change in the structure out to the 34 kt radius. The only significant feature in this panel is the expansion of an area of 22.5 kt winds in the northwest quadrant. The loosening of the pressure gradient, if persistent, could indicate an asymmetry that allows Joaquin to continue to deform in the northwest quadrant.

In the top left panel (0000 UTC 4 October) the 95 kt radius continues to persist (Figure 34). The 80 kt radius has expanded slightly but continues to maintain its position in the southeast quadrant. Based on the surface wind analysis, the eye has undergone considerable deformation and has become elliptical. The area of 22.5 kt winds continues to persist in the northwest quadrant and has continued to expand (not shown). The 64 kt and 50 kt radii have expanded significantly, which indicates that Joaquin has reached maximum intensity. The top right panel (0600 UTC 4 October) is the last panel in which a 95 kt wind radius exists. The other significant difference between 0000 UTC and 0600 UTC is the reduction of the 34 kt radius in the northeast and southwest quadrants. It would appear that Joaquin, having reached maximum intensity, required a compensating relaxation of the outer winds.

The bottom left panel (1200 UTC 4 October) exhibits the first signs that Joaquin is weakening rapidly. The 95 kt radius is absent and the 80 kt radius has decreased significantly. The 64 kt radius has decreased in all four quadrants and

the discontinuity has shifted from the northwest quadrant to the southeast quadrant. This shift is likely in response to the shift of VWS from the northwest to the west while maintaining a magnitude of 12.6 m/s. The 50 kt and 34 kt radii have somewhat decreased, but they remain close to the values at 0600 UTC, which indicates that the weakening is occurring from the inside out.

The bottom right panel (1800 UTC 4 October) does not have an 80 kt radius as Joaquin has continued to weaken. The 64 kt radius has continued to diminish but the discontinuity in the southwest quadrant has shifted farther south in response to the corresponding shift in VWS direction that is now coming from the southwest. The VWS has decreased dramatically at this time to a value of 4.9 m/s (SHIPS). The 50 kt and 34 kt radii have continued to diminish as well.

The last two analyses for Joaquin surface winds show the middle stages of the interrupted rapid decay (Figure 35). In the left panel (0000 UTC 5 October) the 80 kt radius is no longer present. The 64 kt radius has been decimated and is only present in the southwest quadrant, which is a position very similar to the 80 kt radius at 1800 UTC 4 October (Figure 34, bottom right). The 50 kt radius has been reduced again while the 34 kt radius has expanded slightly. In the right panel (0600 UTC 5 October) the 64 kt radius is no longer present and both the 50 kt and 34 kt radii have diminished again. Note that the VWS directions in Figure 22 (top right) are from the southwest and west-southwest and the expected deformations that would occur with the shear are not occurring at this time. Although the VWS magnitudes are still large enough to have an impact on Joaquin, it appears that the deformation that occurred on 4 October (Figure 29) has continued.

Based on the findings of Frank and Ritchie (2001), if there was a surface wind analysis available for 1200 UTC 5 October, there could be a potential increase in surface wind speeds based on the decrease in VWS and the subsequent maintaining intensity exhibited by Hurricane Joaquin in the upper-levels.
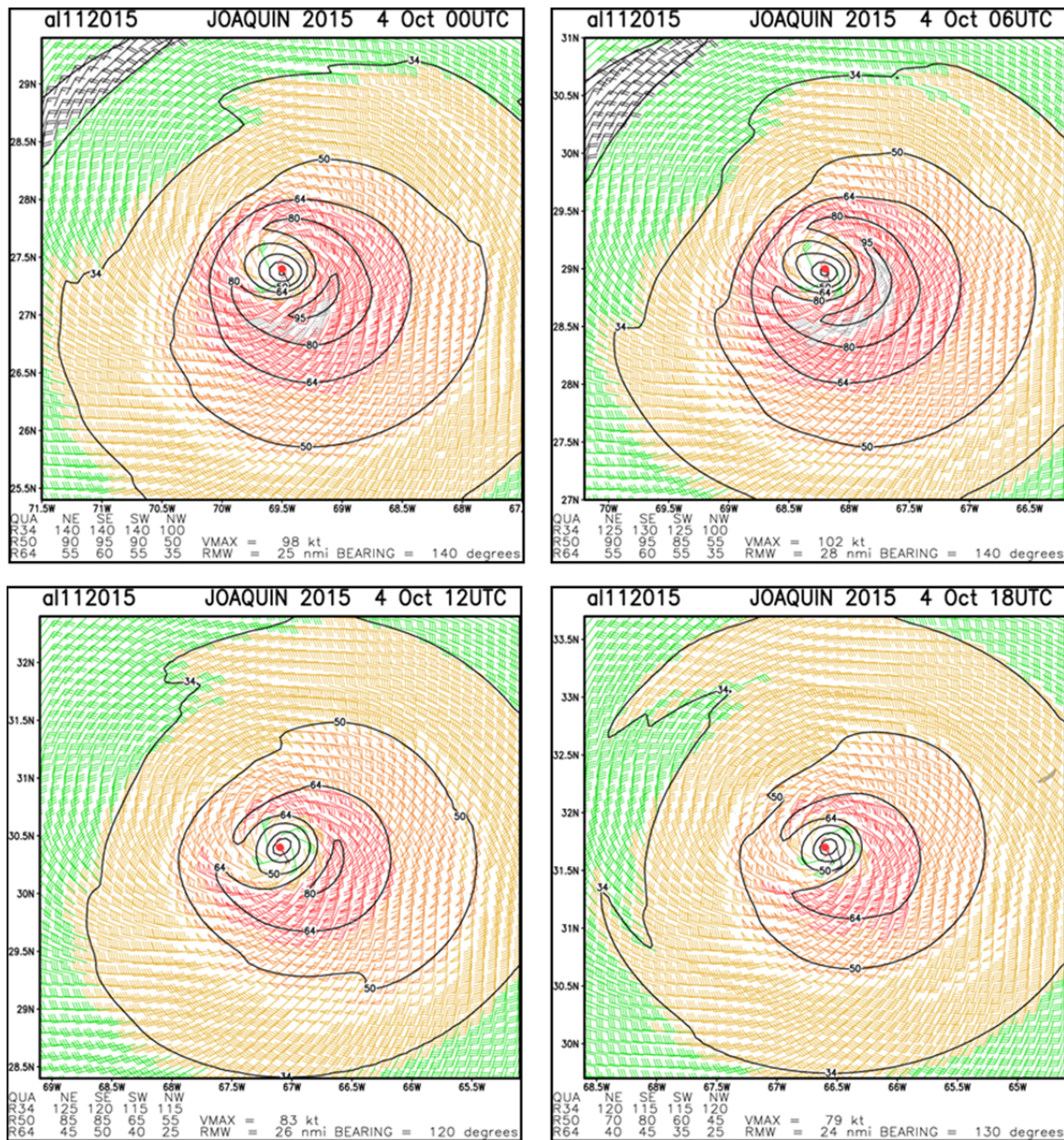
RAMMB compiled surface wind analysis for Hurricane Joaquin at synoptic times. 0000 UTC 4 October (top left) VWS is 95 at 16.5 m/s (CIMSS) and 114 at 8.3 m/s (SHIPS), 0600 UTC 4 October (top right) VWS is 77 at 17 m/s (CIMSS) and 102 at 14.4 m/s (SHIPS), 1200 UTC 4 October (bottom left) VWS is 58 at 13.6 m/s (CIMSS) and 99 at 12.6 m/s (SHIPS), and 1800 UTC 4 October (bottom right) VWS is 54 at 13.3 m/s (CIMSS) and 66 at 4.9 m/s (SHIPS). Wind speed is measured in knots and direction of VWS is degrees. Source: RAMMB Archive. Surface Wind Field for Hurricane Joaquin 4 October

Figure 34.   Surface Wind Field for Hurricane Joaquin 4 October
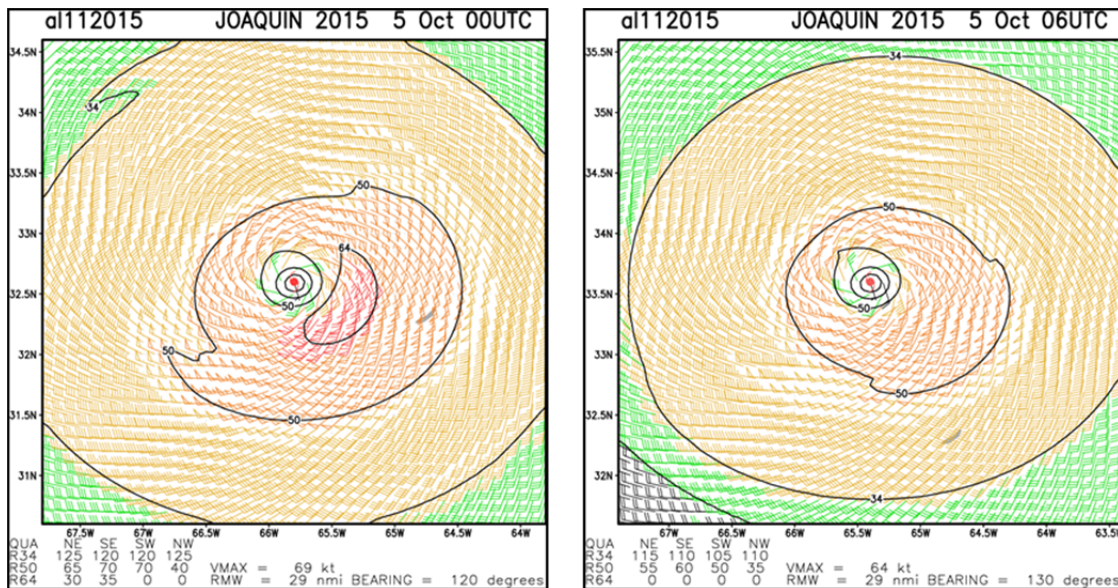
RAMMB compiled surface wind analysis for Hurricane Joaquin at synoptic times. 0000 UTC 5 October (left) VWS is 49 at 12.8 m/s (CIMSS) 34 at 7.4 m/s (SHIPS) and 0600 UTC 5 October (right) VWS is 62 at 8.3 m/s (CIMSS) and 59 at 8.1 m/s. Wind speed is measured in knots and direction of VWS is degrees. Source: RAMMB Archive.

Figure 35.   Surface Wind Field for Hurricane Joaquin 5 October

C.   HURRICANE IMAGING RADIOMETER (HIRAD) DATA

The HIRAD surface wind speed dataset collected during TCI-15 is an additional resource to examine aspects of the vortex and how they respond to the VWS. Due to the broad extent of Hurricane Joaquin, the 50-70 km HIRAD swath may not include the whole inner-core region, but there should be ample high resolution data to draw some conclusions.

The NASA WB-57 completed two passes over the center of Hurricane Joaquin on 3 October (Figure 36). The left panel is the first pass over the storm (1645 UTC 3 October) and the right panel is the second pass over the storm (1824 UTC 3 October). Both passes show a significant asymmetry over the center of the storm. Wind speeds are close to 70 m/s on the east side of the eye while the wind speeds on the west side of the eye are limited to 30 m/s. The RAMMB surface wind analyses for 1800 UTC 3 October (Figure 33, bottom right panel) correlate nicely with the HIRAD imagery (Figure 36). The maximum winds

in both are located in the southeast quadrant, which is the down shear left quadrant that has been observed to be the most active quadrant for both maximum winds and rain rates (Corbosiero and Molinari 2003: DeHart et al. 2014). The rain rate is also significantly asymmetric reaching a maximum of approximately 40 mm/hr in the northeast and southeast quadrants while displaying a significantly drier 15-20 mm/hr in the northwest quadrant in pass 1. The timing of this flight coincides nicely with a maximum SHIPS VWS measured during the storm (13.2 m/s) from the northwest. In Reasor et al. (2004), when VWS begins to tilt the vortex of the TC, eyewall convection becomes asymmetric with a maximum in the down shear quadrant of the storm. This is readily apparent in both of the panels in Figure 36 showing maximum rain rates in the downshear left quadrant of Joaquin as expected from Corbosiero and Molinari's (2003) findings.
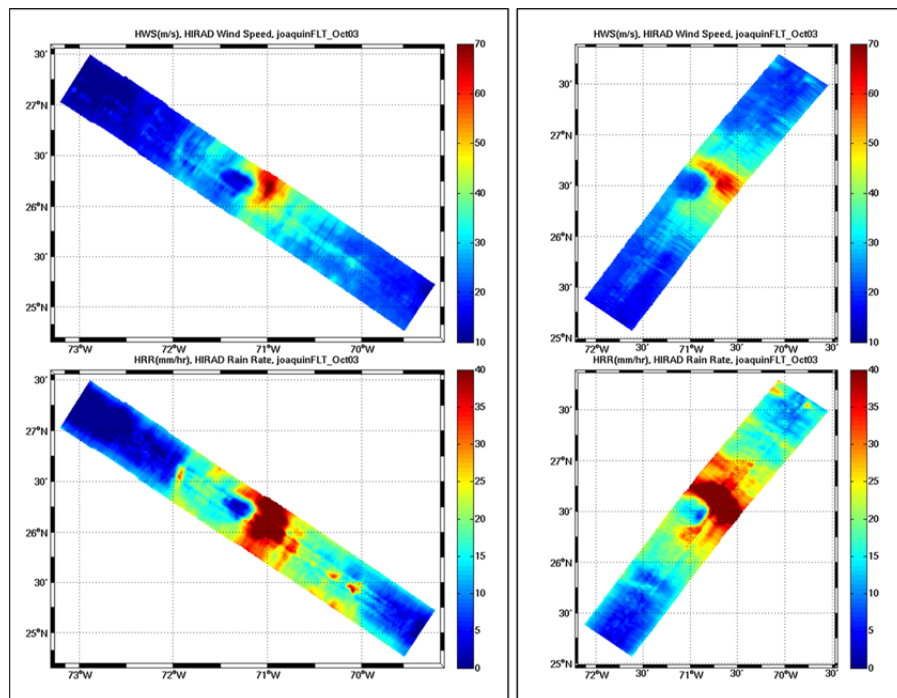
HIRAD data collected by NASA WB-57 flight over Hurricane Joaquin at approximately 1645 UTC 3 October. VWS as of 1800 UTC 3 October is 110 degrees at 18.6 m/s (CIMSS) and 127 degrees at 13.2 m/s (SHIPS). Wind speeds are measured in m/s and rain rate is measured in mm/hr. Source: Cecil et al. (2016)

Figure 36.   HIRAD Wind Speed and Rain Rate for Hurricane Joaquin on 3 October

The NASA WB-57 mission completed another two passes over Joaquin's center on 4 October (Figure 37). The left panel is the first pass over the storm (1817 UTC 4 October) and the right panel is the second pass over the storm (1913 UTC 4 October). There has been a significant shift between mission one and mission two with the HIRAD maximum wind speeds now located in the northeast quadrant as the VWS had shifted to the southwest and slowed considerably (not shown). The maximum winds and rain rate for both passes seem to have spread to encompass down shear (neither right nor left) of the VWS direction which seems to agree with Reasor et al. (2004). The rain rate correlates nicely with the location of the maximum winds on the first pass. The winds are indicated to be considerably weaker during the second pass, but the possibility of background noise eroding the return may be at fault. There is still strong agreement between placement of maximum winds and strongest precipitation with the possible appearance of a rain band approximately 60 nm west of the eye. There appears to be a deformation of the eye occurring between the two passes with the eye becoming more oblong during pass two. The deformation of the eye in conjunction with the location of the wind and precipitation maxima seems to support the VWS shift to the southwest.
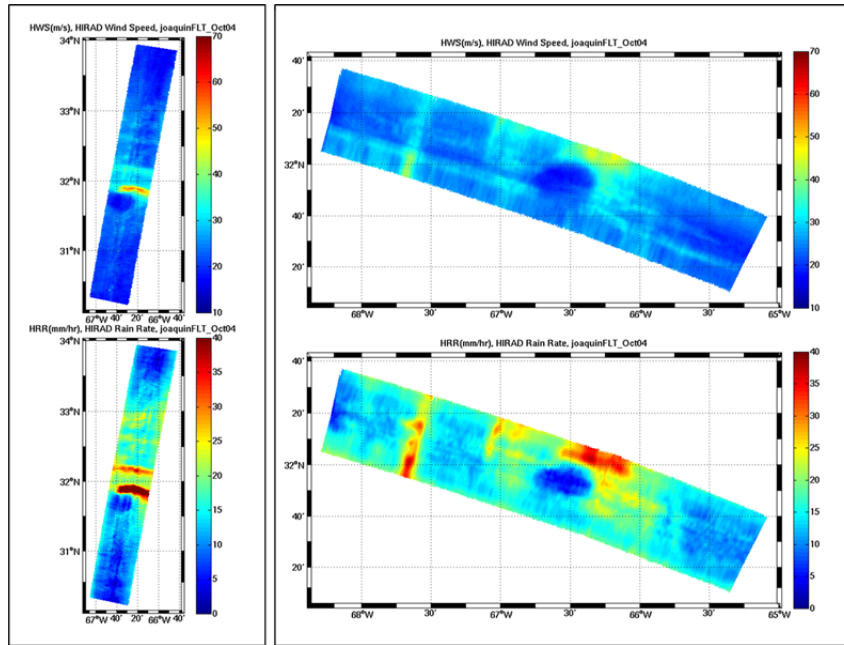
HIRAD data collected by NASA WB-57 flight over Hurricane Joaquin on 4 October. VWS as of 1800 UTC 4 October is 54 degrees at 13.3 m/s (CIMSS) and 66 degrees at 4.9 m/s (SHIPS).Wind speeds are measured in m/s and rain rate is measured in mm/hr. Source: Cecil et al. (2016)

Figure 37.   HIRAD Wind Speed and Rain Rate for Hurricane Joaquin on 4 October

The NASA WB-57 mission completed one pass over Joaquin's center on 5 October (Figure 38). The pass over the storm occurred at 1737 UTC 5 October. The maximum winds as well as the maximum rain rate appear to be in the northwest quadrant but both have decreased significantly between Figure 37 and Figure 38. The maximum winds and rain rate have again aligned themselves in the down shear left quadrant, providing further evidence that at least the inner-core region is behaving as expected in VWS (Rios-Berrios and Torn, 2017). The eye has maintained its oblong shape achieved on 4 October, neither recovering nor deteriorating further. The VWS at the time of this pass was around 4 m/s from the southwest, but the location of Joaquin was conducive only to maintaining intensity, but only for another 12 hours as it began its final decay at 1200 UTC 6 October (Table 1).
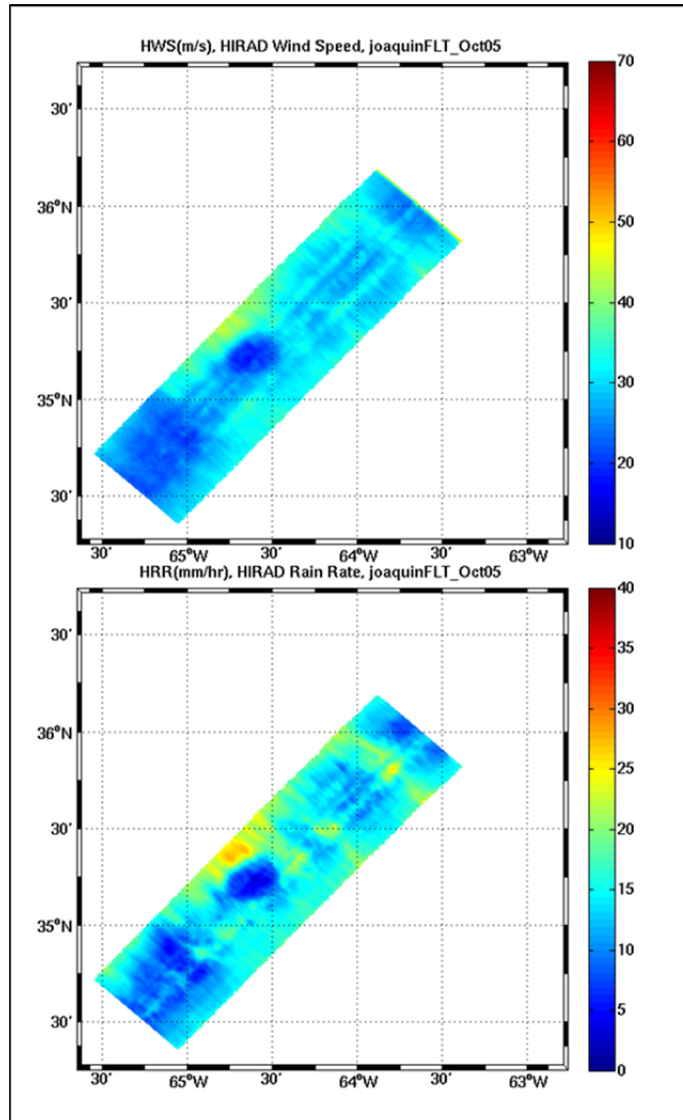
HIRAD data collected by NASA WB-57 flight over Hurricane Joaquin on 5 October. . VWS as of 1800 UTC 5 October is 74 degrees at 8.4 m/s (CIMSS) and 39 degrees at 3.9 m/s (SHIPS). Wind speeds are measured in m/s and rain rate is measured in mm/hr. Source: Cecil et al. (2016)

Figure 38.   HIRAD Wind Speed and Rain Rate for Hurricane Joaquin on 5 October

## D.	SYNTHESIS

According to the ZWC tool (Creasey and Elsberry 2017) the interruption of the rapid decay of Joaquin was based on the relaxation of VWS to allow the storm to become more vertically stacked (Figure 30). The evolution of the surface wind analyses from RAMMB seem to support this from the surface and the aspects of the vortex investigated using HIRAD data from the Earth Observing Laboratory (EOL) also point to agreement that the relaxation of VWS extended the life-time of Hurricane Joaquin. Another interesting aspect of this analysis is the rapid variations in tilt at different levels of Joaquin as it is responding to VWS, which indicates the complex process by which Joaquin responded to environmental shear that deserves further research.

THIS PAGE INTENTIONALLY LEFT BLANK

VI. CONCLUSIONS

This thesis utilized environmental analysis data, CIMSS 6-hourly and special 15-minute VWS datasets calculated from rapid-scan atmospheric motion vectors, TCI-15 field experiment HDSS and HIRAD data, RAMMB surface wind analyses, and ZWC calculations (Creasey and Elsberry 2017) based on HDSS data to investigate the environmental factors and internal processes that led to the interrupted rapid decay of Hurricane Joaquin. The VWS calculations provided a detailed look at the VWS environment that Joaquin was exposed to during the interrupted rapid decay. The HDSS data was utilized to compute the ZWCs to investigate the vortex response to the VWS in terms of the tilt, and the relationship to the interrupted rapid decay. The RAMMB surface wind analyses (RAMMB 2017) and HIRAD (Cecil et al. 2016) surface wind speed and rain rates were utilized to understand the low level wind structure response of the storm to the VWS.

With the exception of VWS, all environmental factors examined were negative, and thus cannot explain the interrupted rapid decay of Joaquin. The SST was not high enough, the divergence aloft was too weak, and the relative humidity in the mid-levels was too low. However, in both the 6-hourly and 15-minute datasets of the CIMSS VWS with the vortex removed, the VWS magnitude decreased from more than 15 m/s during the period of rapid decay to a more moderate (8 m/s) VWS at the time of interrupted rapid decay of Hurricane Joaquin and maintenance of a constant intensity for about 30 hours. Thus, the main conclusion is that the weakening of the VWS was likely significant enough to cause the interrupted rapid decay of Joaquin, even though all other environmental factors were negative. This illustrates how critical VWS can be for TC intensity in comparison to other environmental factors. The special CIMSS 15-minute VWS dataset was invaluable to the research conducted in this thesis as it allowed for a high temporal resolution analysis of VWS during this critical interrupted decay period. The contour plots in chapter IV displayed a mesoscale

event (Joaquin) moving through a synoptic environment and shed light on how that synoptic environment interacted with Joaquin on a time scale that fills in the gaps between the synoptic time calculations. The 15-minute dataset should provide modelers the opportunity to ingest high temporal resolution VWS values which should refine the model's ability to handle the dynamic VWS environment.

On investigation of the internal processes, the ability for Hurricane Joaquin to re-align itself in the lower to mid troposphere strongly supports the idea of vortex resiliency (Reasor et al. 2004). The relaxation of the VWS around that time likely aided Joaquin in the interruption of rapid decay. The evolution of the surface winds from RAMMB seem to support this from the surface and the aspects of the vortex investigated using HIRAD data from the Earth Observing Laboratory (EOL) also point to agreement with the relaxation of VWS extending the life time of Hurricane Joaquin.

Based on the analysis of the last two chapters, the conclusion drawn by this thesis is that the relaxation of VWS provided Hurricane Joaquin the opportunity to make a vertical adjustment that significantly extended the life time of the storm.

LIST OF REFERENCES

Berg, R., 2016: National Hurricane Center tropical cyclone report: Hurricane Joaquin (AL112015). Accessed 01 May 2017. [Available online at http://www.nhc.noaa.gov/data/tcr/AL112015_Joaquin.pdf.]

Black, P., L. Harrison, M. Beaubuen, R. Bluth, R. Woods, A. Penny, R. W. Smith, and J. D. Doyle, 2017: High-Definition Sounding System (HDSS) for atmospheric profiling. *J. Atmos. Oceanic Technol.*, **34**, 777–796, doi: 10.1175/JTECH-D-14-00210.1.

Bosart, L. F., C. S. Velden, W. E. Bracken, J. Molinari, and P. G. Black, 2000: Environmental influences on the rapid intensification of Hurricane Opal (1995) over the Gulf of Mexico. *Mon. Wea. Rev.*, **128**, 322–352.

Cecil, D., S. Biswas, W. Jones, and F. Alquaied, 2016: Hurricane Imaging Radiometer (HIRAD) data. UCAR/NCAR–Earth Observing Laboratory, Accessed 02 May 2017, doi:10.5065/D6CF9NGC.

Corbosiero, K. L., and J. Molinari, 2002: The effects of vertical wind shear on the distribution of convection in tropical cyclones. *Mon. Wea. Rev.*, **130**, 2110–2123.

Creasey, R. L., and R. L. Elsberry, 2016: Tropical cyclone center positions from sequences of HDSS sondes deployed along high-altitude overpasses. *Wea. Forecasting*, **32**, 317–325, doi: 10.1175/WAF-D-16-0096.1.

Davis, C., and J. Chan, 2014: Report 14.1. Tropical cyclone intensification: prediction and mechanisms. *World Weather Open Science Conference 2014*, Montreal, Canada, WWOSC. [Available online at https://www.wmo.int/pages/prog/arep/wwrp/new/documents/Chapter14_TropicalCyclones.pdf.]

DeHart, J. C., R. A. Houze, and R. F. Rogers, 2014: Quadrant distribution of tropical cyclone inner-core kinematics in relation to environmental shear. *J. Atmos. Sci.*, **71**, 2713–2732, doi: 10.1175/JAS-D-13-0298.1

DeMaria, M., and J. Kaplan, 1993: Sea surface temperature and the maximum intensity of Atlantic tropical cyclones. *J. Climate.*, **7**, 1324–1334.

DeMaria, M., 1996: The effect of shear on tropical cyclone intensity change. *J. Atmos. Sci.*, **53**, 2076–2087.

DeMaria, M., M. Mainelli, L. K. Shay, J. A. Knaff, and J. Kaplan, 2005: Further improvements to the Statistical Hurricane Intensity Prediction Scheme (SHIPS). *Wea. Forecasting*, **20**, 531–543.

Doyle, J. D., and Coauthors, 2017: A view of tropical cyclones from above: The Tropical Cyclone Intensity (TCI) Experiment. *Bull. Amer. Meteor. Soc.*, doi: 10.1175/BAMS-D-16-0055.1.

Elsberry, R. L., and R. A. Jeffries, 1996: Vertical wind shear influences on tropical cyclone formation and intensification during TCM-92 and TCM-93. *Mon. Wea. Rev.*, **124**, 1374–1387.

Elsberry, R. L., M. Bell, B. Creasey, E. A. Hendricks, D. Ryglicki, and C. Velden, 2016: Environmental and internal physical processes during the interrupted rapid decay of hurricane Joaquin. *Tropical Cyclone Intensity (TCI) Workshop*, Boulder, CO.

Finocchio, P. M., S. J. Majumdar, D. S. Nolan, and M. Iskandarani, 2016: Idealized tropical cyclone responses to the height and depth of environmental vertical wind shear. *Mon. Wea. Rev*, **144**, 2155–2175, doi: 10.1175/MWR-D-15-0320.1

Frank, W. M. and E. A. Ritchie, 2001: Effects of vertical wind shear on the intensity and structure of numerically simulated hurricanes. *Mon. Wea. Rev.*, **129**, 2249–2269.

Gray, W. M., 1968: Global view of the origin of tropical disturbances and storms. *Mon. Wea. Rev.*, **96**, 669–700.

Hendricks, E. A., M. S. Peng, B. Fu, and T. Li, 2010: Quantifying environmental control on tropical cyclone intensity change. *Mon. Wea. Rev.*, **138**, 3243–3271.

Hill, K. A., and G. M. Lackmann, 2009: Influence of environmental humidity on tropical cyclone size. *Mon. Wea. Rev.*, **137**. 3294–3315, doi: 10.1175/2009MWR2679.1

Jones, S. C., 1995: The evolution of vortices in vertical shear. I: Initially barotropic vortices. *Quart. J. Roy. Meteor.*, **121(524)**, 821–851, Doi:10.1002/qj.49712152406.

Nyoumura, Y., and H. Yamashita, 1984: On the central pressure change of tropical cyclones as a function of sea surface temperature and land effect. *Geophys. Mag.* **41**, 45–59.

Park, M. S., R. L. Elsberry, and P. A. Harr, 2012: Vertical wind shear and ocean heat content as environmental modulators of western north Pacific tropical cyclone intensification and decay. *Tropical Cyclone Research and Review*. **1**, 448–457.

RAMMB, 2017: Real-time tropical cyclone products–description of products. CIRA, 01 June 2017, http://rammb.cira.colostate.edu/products/tc_realtime/about.asp.

Rappin, E. D., M. C. Morgan, and G. J. Tripoli, 2011: The impact of outflow environment on tropical cyclone intensification and structure. *J. Atmos. Sci.*, **68**, 177–194.

Reasor, P. D., M. T. Montgomery, and L. D. Grasso, 2003: A new look at the problem of tropical cyclones in vertical shear flow: vortex resiliency. *J. Atmos. Sci.*, **61**, 3–22.

Rhome, J. R., C. A. Sisko, and R. D. Knabb, 2006: On the calculation of vertical shear: An operational perspective, extended abstract. *27th Conference on Hurricanes and Tropical Meteorology,* Monterey, CA, Amer. Meteor. Soc., 14A.4. [Available online at https://ams.confex.com/ams/27Hurricanes/techprogram/paper_108724.htm].

Riemer, M., M. T. Montgomery, and M. E. Nicholls, 2010: A new paradigm for intensity modification of tropical cyclones: thermodynamic impact of vertical wind shear on the inflow layer. *Atmos. Chem. Phys.*, **10**, 3163–3188.

Tang, B., and K. Emanuel, 2010: Midlevel ventilation's constraint on tropical cyclone intensity. *J. Atmos. Sci.*, **67**, 1817–1830, doi: 10.1175/2010JAS3318.1.

Velden, C. S., and J. Sears, 2014: Computing deep-tropospheric vertical wind shear analyses for tropical cyclone applications: Does the methodology matter? *Wea. Forecasting*, **29**, 1169–1180, doi: 10.1175/WAF-D-13000147.1.

Willoughby, H. E., and M. B. Chelmow, 1982: Objective determination of hurricane tracks from aircraft observations. *Mon. Wea. Rev.*, **110**, 1298–1305.

THIS PAGE INTENTIONALLY LEFT BLANK

INITIAL DISTRIBUTION LIST

1.   Defense Technical Information Center
        Ft. Belvoir, Virginia

2.   Dudley Knox Library
        Naval Postgraduate School
        Monterey, California